Environmental and Molecular Mutagenesis 00:00–00 (2016)

Research Article

A Multi-Ingredient Dietary Supplement Abolishes Large-Scale Brain Cell Loss, Improves Sensory Function, and Prevents Neuronal Atrophy in Aging Mice

AQ3 J.A. Lemon,[1]* V. Aksenov,[2] R. Samigullina,[2] S. Aksenov,[3] W.H. Rodgers,[3] C.D. Rollo,[2] and D.R. Boreham[1,4]

[1]Department of Medical Physics and Applied Radiation Sciences
[2]Department of Biology, McMaster University, Hamilton, Ontario, Canada
[3]Department of Pathology, New York-Presbyterian/Queens Hospital, Flushing, New York
[4]Medical Sciences Division, Northern Ontario School of Medicine, Sudbury, Ontario, Canada AQ1

Transgenic growth hormone mice (TGM) are a recognized model of accelerated aging with characteristics including chronic oxidative stress, reduced longevity, mitochondrial dysfunction, insulin resistance, muscle wasting, and elevated inflammatory processes. Growth hormone/IGF-1 activate the Target of Rapamycin known to promote aging. TGM particularly express severe cognitive decline. We previously reported that a multi-ingredient dietary supplement (MDS) designed to offset five mechanisms associated with aging extended longevity, ameliorated cognitive deterioration and significantly reduced age-related physical deterioration in both normal mice and TGM. Here we report that TGM lose more than 50% of cells in midbrain regions, including the cerebellum and olfactory bulb. This is comparable to severe Alzheimer's disease and likely explains their striking age-related cognitive impairment. We also demonstrate that the MDS completely abrogates this severe brain cell loss, reverses cognitive decline and augments sensory and motor function in aged mice. Additionally, histological examination of retinal structure revealed markers consistent with higher numbers of photoreceptor cells in aging and supplemented mice. We know of no other treatment with such efficacy, highlighting the potential for prevention or amelioration of human neuropathologies that are similarly associated with oxidative stress, inflammation and cellular dysfunction. Environ. Mol. Mutagen. 00:000–000, 2016. © 2016 Wiley Periodicals, Inc.

Key words: aging; neurodegeneration; multi-ingredient dietary supplement; oxidative stress; neuroprotectant

INTRODUCTION

The brain is particularly vulnerable to free radical damage with its high content of unsaturated fatty acids, high oxygen metabolism (20% of total body consumption) and relatively low levels of endogenous antioxidants. Accumulation of oxidative damage in post-mitotic neurons is a crucial factor in normal brain aging, and contributes directly to cognitive, motor and sensory impairments [Antier et al., 2004; Mattson and Magnus, 2006; Wang and Michaelis, 2010; Yin et al., 2014]. This appears to be exacerbated in many neurodegenerative diseases, many of which are also associated with aging [Markebury and Carney, 1999, Butterfield et al., 2001; Ma et al., 2003; Butterfield, 2014].

Mitochondrial dysfunction and oxidative metabolism are principal sources of oxidative stress leading to neurodegeneration, although NAD(P)H oxidase and other sources of free radicals also contribute [Rollo, 2002; Sonta et al., 2004; Cui et al., 2012; Gandhi and Abramov, 2012]. Neurons have high energy demands (ATP

Grant sponsor: National Sciences and Engineering Research Council of Canada, Bruce Power and the CBRN Research and Technology Initiative.

*Correspondence to: Dr. Jennifer Lemon, McMaster University, 1280 Main Street West, Hamilton, ON, L8S 4K1. E-mail: lemonja@mcmaster.ca

Received 30 November 2015; provisionally accepted 14 April 2016; and in final form 00 Month 2016

DOI 10.1002/em.22019

Published online 00 Month 2016 in Wiley Online Library (wileyonlinelibrary.com).

Environmental and Molecular Mutagenesis. DOI 10.1002/em

consumption) associated with membrane ionic pumps, channel activity, and synaptic transmission [Erecinska et al., 2004; Du et al., 2008], which can lead to increased free radical production. Elevation in free radicals can increase levels of glutathione disulfide (GSSG) which inhibits the thiol-dependent enzyme NADH dehydrogenase, causing a mitochondrial complex I defect [Cohen et al., 1997]. Mitochondrial dysfunction can lead to neuronal degeneration via impaired production of ATP (through disruption of the electron transport chain (ETC)), increased generation of reactive oxygen species (ROS), altered calcium homeostasis and excitotoxicity [Shigenaga et al., 1994, Lenaz, 1998; Sastre et al., 2003; Reddy and Beal, 2008; Hattingen et al., 2009; Bratic and Larsson, 2013; Yan et al., 2013]. Brains of aged animals have significantly higher levels of oxidized proteins and lipids, and reduced protease activities compared to young animals [Keller et al., 1997; Dei et al., 2002; Grimm et al., 2011].

Age-related functional loss is not limited to cognition and physical activity. Aging is associated with rapid deterioration of sensory and somatosensory functions including vision, olfaction, and motor coordination [Wallace et al., 1980; Cain and Stevens, 1989; Spear, 1993; Foster et al., 1996; Bickford et al., 1999; Nakayasu et al., 2000; Rawson, 2006]. While not inherently fatal these conditions are associated with substantially elevated morbidity and mortality [Schiffman et al., 1990; Struble and Clark, 1992; Ter Laak et al., 1994; Devanand et al., 2000; Girardi et al., 2001; Schiffman et al., 2002; Tan et al., 2008; Li et al., 2010; Baba et al., 2012; Doty, 2012], and obvious impacts on quality of life.

Age-related deterioration of motor coordination is a major cause of falls in the elderly, exacerbated by balance, arthritis, and declining physical strength [Girardi et al., 2001]. Olfaction is of unique clinical importance, as olfactory deficits precede and accurately predict onset of debilitating neurodegenerative conditions such as dementia, Alzheimer's and Parkinson's [Struble and Clark, 1992; Devanand et al., 2000; Schiffman et al., 1990, 2002; Li et al., 2010; Ter Laak et al., 1994; Baba et al., 2012; Doty, 2012].

Regardless of the current debate regarding the free radical theory of aging, we predicted a priori that our transgenic rat growth hormone mouse (TGM) would express elevated free radical processes and that these would be correlated to aging rates. Subsequent examination of lipid peroxidation (LP) and superoxide radical (SO) found elevated free radical processes in all tissues examined, particularly the brain [see Rollo et al., 1996; Carlson et al., 1999; Hauck and Bartke, 2001]. Levels of SO and LP also increased with age and was highly correlated to longevity [Rollo et al., 1996]. TGM are substantially larger than normal mice (Fig. 1A), have reduced lifespan (50% of normal siblings), early mitochondrial deterioration, accelerated kidney and liver disease, and early onset of symptoms resembling normal murine aging (Fig. 1B) [Steger et al., 1993; Wolf et al., 1993; Meliska et al., 1997; Ogueta et al., 2000]. These include reduced cellular replicative potential, early reproductive senescence, increasing tissue oxidative and nitrosative damage, arthritis, reduced motor activity, cataracts, sarcopenia, kyphosis, and altered fur quality [Bartke et al., 2002; Bartke, 2003; Lemon et al., 2005; Aksenov et al., 2010, 2013; Long et al., 2012].

Young TGM (<7 mo.) have vastly superior cognition than normal mice, learning an eight-choice radial maze in roughly half the trials required by age-matched normal mice (many of which did not learn at all) [Rollo et al., 1999; Lemon et al., 2003]. However, cognitive abilities of TGM rapidly deteriorated and by 11 months of age, most were unable to learn the maze. The performance of normal mice is essentially unchanged across the same age range [Lemon et al., 2003; Long et al., 2012; Aksenov et al., 2013]. Increasing levels of ROS, low-level inflammation, impaired energy supply, loss of membrane fluidity and mitochondrial dysregulation are all common features of normal brain aging and neuropathologies [Lyras et al., 1997; Mattson et al., 1999; Butterfield et al., 2001; Mutlu-Turkoglu et al., 2003; Sastre et al., 2003; Antier et al., 2004]. We hypothesized that an intervention targeting multiple cellular processes might ameliorate premature aging in TGM and associated pathologies. Specific development and testing of multipurpose, multi-ingredient supplements is lacking. Most scientific studies examine one or only a few ingredients at a time (usually antioxidants or anti-inflammatories), which precludes obtaining the benefits of synergistic or interactive effects which may emerge in more complex formulations. We employed a multiple ingredient dietary supplement (MDS) designed to specifically target five critical processes associated with aging [Lemon et al., 2003, Aksenov et al., 2010, 2013, Long et al., 2012]. Ingredients and dosages have been described [Lemon et al., 2003, 2005]. The dietary supplement completely abolished the age-related cognitive decline in TGM. Remarkably, MDS supplemented older TGM had significantly better maze performance than younger control TGM and more than 2-fold faster task learning than normal mice. TGM cognitive decline was not only prevented, but augmented by the MDS. The MDS supplement also benefited older normal mice (>24 mo.) [Lemon et al., 2003, Long et al., 2012, Aksenov et al., 2013]. Increases in mean and maximal longevity were also observed in supplemented TGM and normal mice [Lemon et al., 2005]. Even in advanced ages, MDS supplemented mice exhibited youthful cognitive and motor abilities [Lemon et al., 2003, 2005, Aksenov et al., 2010, 2013]. While intensity of physical activity was reduced with age, the duration of daily locomotion was unchanged from youth well into oldest ages (Aksenov

J_ID: z8i Customer A_ID: EM22019 Cadmus Art: EM22019 Ed. Ref. No.: EMM-15-0117.R1 Date: 29-April-16 Stage: Page: 3

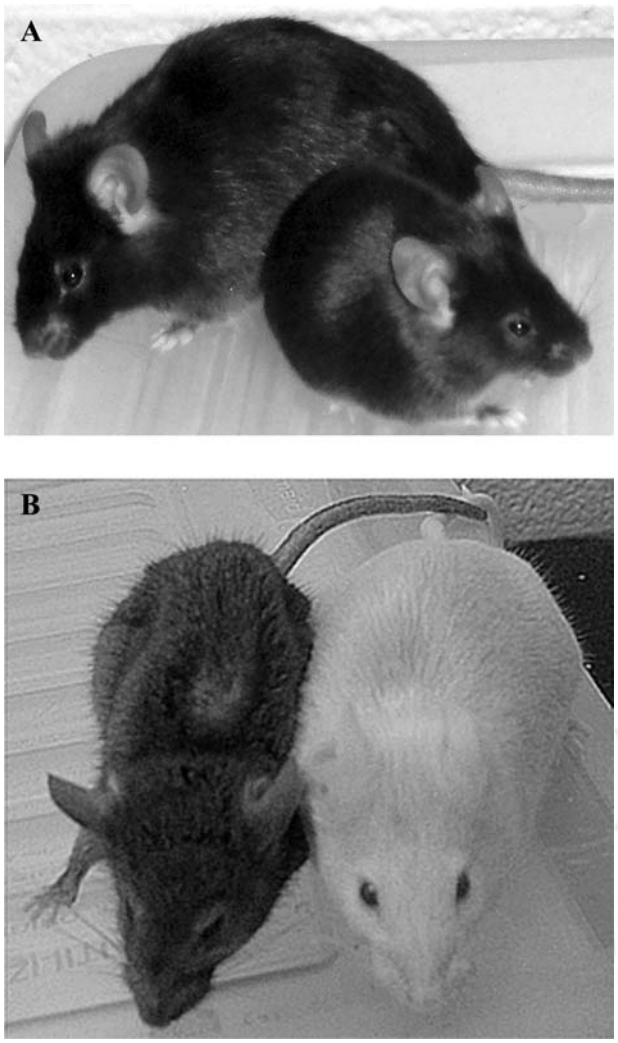

Fig. 1. **A**: Young adult TGM (left side) and normal mouse (age-matched) illustrates typical body size difference between strains, **B**) 12-month-old TGM (diet supplemented mouse on right) displaying dramatic improvement of body condition in supplemented old TGM; note difference in hunching, fur quality and wasting (coat colour is not related to trans gene or supplement).

et al., 2010). Thus, mice appear to retain the capacity for youthful cognitive functionality, and to a large degree, youthful motor abilities into advanced ages. Improved cognition and physical abilities in supplemented animals were attributed to reduced oxidative and nitrosative damage and enhanced mitochondrial activity in MDS treated animals [Lemon et al., 2003; Aksenov et al., 2010; Long et al., 2012].

In previous work, we showed that age-related cognitive and motor declines could be prevented or delayed by dietary supplementation. We postulated that, due to the chronic oxidative stress experienced by TGM, increased brain cell loss, likely through apoptosis, was a likely mechanism underlying dramatic age-related cognitive decline. Given that the MDS abolishes the early cognitive decline in TGM, we speculated there would be a reduction in apoptotic cell loss in older TGM on the dietary supplement. In the present work, we also examined whether benefits of the MDS extended to sensory and behavioral function in aging mice. Mice were subjected to a battery of tests to assess motor coordination, vision, olfaction, emotionality and contextual discrimination. Remarkably, MDS supplemented mice showed significant improvements on virtually all aspects examined.

MATERIALS AND METHODS

Animals

Heterozygous TGM males were mated to normal (Nr) females yielding equal numbers of TGM and Nr offspring of similar genetic background. Heterozygote TGM were distinguishable from their normal littermates by their larger size and phenotypic alterations at 28 d of age. Mice were maintained in standard housing cages on a 12 : 12 h light:-dark photoperiod at 22 ± 2°C. Food and water were supplied ad libitum. Lifespan of our untreated Nr and TGM mice are consistent with published lifespan of this mouse strain [Hauke et al., 2001; Bartke et al., 2003; Lemon et al., 2008]. All procedures and protocols were approved by McMaster University Animal Research Ethics Board and adhered to the Canadian Council on Animal Care. Genders, genotypes, ages and numbers of mice used in various studies are indicated as appropriate.

Multi-Ingredient Dietary Supplement

The MDS was designed to simultaneously ameliorate key processes implicated in aging (oxidative stress, inflammatory processes, insulin resistance, and membrane and mitochondrial deterioration). Materials were chosen based on documented effectiveness for one or more of the targeted features and could be safely taken orally. Dosages for the mice were reformulated based on amounts commonly recommended for humans. Dosages were adjusted for the smaller body size of the mice and increased by a factor of 10 based on the higher gram-specific metabolic rate (and consequently faster utilization and turnover) of mice compared to humans [Calder, 1984]. Biological actions of individual components have been previously summarized [Lemon et al., 2008]. The supplement was prepared in liquid form and a 0.4ml volume was soaked into a 1 cm x 1.5 cm x 1 cm piece of bagel and allowed to dry. Each mouse received 1 piece of dried bagel with or without MDS, daily (midway through the photoperiod). The bagel pieces were rapidly eaten by the mice within 20 min, ensuring mice obtained full and equivalent doses. The formulation of the supplement has been previously published [Lemon et al., 2003, 2005] and was maintained for the duration of the study. At weaning mice were randomly assigned to either MDS supplemented or untreated group. MDS mice were treated daily from weaning throughout the lifespan of the animals.

Somatosensory Tests

The severity of age-related losses in motor coordination and overall mobility of older TGM mice makes quantification of somatosensory deficits difficult to delineate from impaired motor function [Lemon et al., 2005], as such all somatosensory tests were conducted on Nr males and females up to 2 years old.

Landing Response

Mice were held by the base of the tail and lowered onto a flat surface, 3cm short of contact. Mice with intact vestibular function extend their forepaws in anticipation of landing.

ID: nagarajulum Time: 13:42 I Path: //chenas03/Cenpro/ApplicationFiles/Journals/Wiley/EM##/Vol00000/160017/Comp/APPFile/JW-EM##160017

Environmental and Molecular Mutagenesis. DOI 10.1002/em

Negative Geotaxis

Similar to the landing response, this test assesses vestibular function [Szechtman, 1988]. Mice were placed on a 30° inclined plane facing down. Mice with uncompromised vestibular function quickly orient their body position to face upward.

Visual Placing

This test has been used previously to grossly assess vision [Chaudhry et al., 2008]. Mice held by the base of the tail were lowered past a black table edge, far enough to prevent vibrissae contact. Mice with intact vision reach for the table edge with their front paws.

Visual Acuity

Based on the principle underlying the visual placing test, a more precise assay for measuring visual acuity was developed. Instead of a single visual cue, this test uses an array of increasingly more challenging visual cues. Mice were suspended by the base of the tail and repeatedly lowered past a black horizontal wire at a distance of 5cm (to avoid vibrissae contact). If able to see the wire, mice reached towards it with the forepaws. Lack of a reaching response on five consecutive attempts indicated that mice were unable to see the wire. The next set of challenges consisted of decreasing wire thickness, background contrast (i.e., white or black background) and room lighting. Specifically, mice were challenged in bright illumination with: (a) 5 mm wire suspended over white background, (b) 5 mm wire suspended over black background, (c) 1 mm wire suspended over black background, (d) 0.5 mm wire suspended over black background, (e) 0.5 mm wire suspended over black background in dim light, and (f) 0.5 mm wire suspended over black background in near darkness. Mice were tested in order of least to most challenging test with 30 min inter-trial intervals.

Olfactory Sensitivity

Test protocols were adopted from Witt et al., [2009]. Three serial dilutions were prepared by diluting 1.25, 2.50, and 5.00 mg of peanut butter in mineral oil to a final volume of 100 ml. A fourth blank dilution (mineral oil only) was used as a negative control. Mice were placed individually placed in a 28 × 16 × 12 cm plastic enclosure and acclimated for 30 min. A camera was set up to record behavior. Just prior to starting a trial, 1 ml of a peanut butter dilution was pipetted onto a 3 × 3 cm filter paper square. The filter paper was sealed inside a small Petri dish with several round holes to allow dispersal of scent and placed in the enclosure. Each mouse was tested on all four peanut butter dilutions in a random order with 2–3 days in between trials. Olfactory sensitivity was assessed by scoring the time spent exploring the Petri dish (e.g., sniffing, licking, biting) in a 10 min time interval. All behavior was video recorded from above.

Pinch Reflex

Mice were lightly pinched by the hind paw. Mice with normal pain sensation and reflexes immediately withdraw the paw.

Behavioral Experiments

Behavioral experiments were performed on both Nr and TGM mice with ages representing the lifespan of the both groups of mice.

Open Field

The bright open field test was previously applied to assess emotionality [Chaudhry et al., 2008]. A square arena 70 cm (w)×70 cm (l)×45 cm (h) constructed from white Plexiglas was illuminated by two 100 W white lightbulbs. A 50 × 50 cm square in the middle and the 10cm wide outside border constituted "central" and "peripheral" zones, respectively. Mice were placed individually in the central zone and videotaped from above for 5 min. Arena was cleaned with ethanol between runs to remove any scent trails from previous trials. Image tracking software (Noldus Ethovision®) was used to score variables: (a) latency to exit central zone, (b) distance traveled in central zone (c) distance traveled in peripheral zone, and (d) mean running velocity.

Step-Down Test

Mice were placed individually on top of a circular 10cm diameter platform, 7 cm high. Initially, trials were conducted in bright illumination (two 100 W white lights), the test was repeated in dim lighting (single 25 W red light), with one week between tests. Latency to step down was recorded with a 10-min time limit.

Circle Run

This test was developed in our lab and was used to assess emotionality in mice [Chaudhry et al., 2008]. Mice have an aversive response to bright, open areas, eliciting anxiety-like behavior; whereas dim illumination allows for observation of active or exploratory behavior [Trullas and Skolnick, 1993; Chaudhry et al., 2008]. A circular white arena 1 m in diameter was surrounded by a shaded overhang 5 cm high and 20 cm wide. A 7 cm diameter, 5 cm deep depression was fitted in the center of the arena. Each mouse was placed in the depression and videotaped from above, latency to climb out of cup with four paws, followed by latency to reach the shaded overhang were scored. Mice were tested on two separate trials, two weeks apart, first in bright, and then in dim illumination.

Rotarod

This standard test assesses motor coordination and balance [Carter et al., 2001]. Mice were individually placed on a horizontal 6cm diameter plastic cylinder, rotating at 12 rev/min. Latency to fall onto a cushioned landing pad was scored on three consecutive trails. Improvement was assessed by subtracting latency to fall on first trial from the latency on the last trial.

Cerebellum, Olfactory Bulb, and Retinal Histology

In mid-photophase, untreated ($n = 6$) and MDS supplemented ($n = 6$) mice, aged 14–17 months were decapitated and brains and eyes were removed. Cerebellum and olfactory bulbs were separated. All tissues were placed in 10% formalin solution, processed overnight and embedded onto paraffin blocks. Tissues were sliced at 5 μm on a microtome and stained with H&E and Nissl stain.

Cerebellum

Thickness of molecular layer and granule cell layer was assessed in Lobules II and III using ImageJ software. Number of Purkinje cells in Lobules II and III were counted. Some studies estimated total cerebellar cellularity by interpolation of counts from an array of sections spanning the entire width of the cerebellum [Woodruff-Pak, 2006]. However, we were only interested in the relative difference between treatment groups; hence, a single representative inter-hemispheric sagittal section was sufficient [Rogers et al., 1984].

Retina

Mid-sagittal sections of eye were used to measure the thickness of the outer nuclear layer and the outer fragment layer in retina. Age-related loss of photoreceptors is most prominent in the central retinal portions; therefore, measurements were performed on retinal cross-

sections 1,000 μm inferior and superior to the position of optical nerve attachment.

Olfactory Bulb

One olfactory bulb from each animal was randomly chosen. Thickness of the glomerular layer, external plexiform layer and counts of mitral cells were performed. Strict criteria were employed in the identification of mitral cells in the olfactory bulb (refer to Fig. 13 caption).

Brain Collection and Preparation for Apoptosis, Cell Counts

Fifty-two mice were used for brain weight assessment. Mice were assigned to one of 16 experimental groups. The mice were divided by the following criteria (n = 3-4/group); age: consisting of mice aged 3-4 months or mice aged 11-12 months (old based on TGM lifespan of 12 months, but middle-aged for normal mice), genotype: TGM or normal isogenic control mice, and treatment: standard rodent chow or standard chow plus MDS. The brains used for the brain weight study were harvested and immediately weighed on a precision balance (AB204-S, Mettler Toledo, Mississauga ON), placed in a cryovial (Nalge Nunc International, Rochester NY), flash frozen in liquid nitrogen and stored at −80°C. To determine if the apparent weight discrepancy in old untreated TGM was due to cell loss by increased apoptosis, the brains of 48 mice were harvested for apoptosis and brain cell density study, n = 3 in the same 16 experimental groups. The brains were harvested, cut in half along the longitudinal axis and placed in 10% neutral buffered formalin within 2 min of dissection. The brain tissue was left in the fixative and stored at room temperature for a minimum of one week prior to embedding in paraffin. The brains were sectioned sagittally from the longitudinal cerebral fissure in 10 μm thick sections using a rotary microtome (Riechert Scientific Instruments, Buffalo NY). Sequential tissue slices were placed on microscope slides, from one side of the longitudinal axis for each mouse covering lateral 0.15 to 0.85.

Apoptosis and Cell Density

Slides were prepared following the protocol provided in the Apoptag® Fluorescein kit (Serologicals, Temecula CA). Briefly, the tissue sections were deparaffinized using xylene, followed by an ethanol rehydration and 1 wash in room temperature phosphate buffered solution (PBS; 137 mM NaCl, 2.7 mM KCl, 4.3 mM Na_2HPO_4, 1.4 mM $KH2PO_4$). The tissue was then pre-treated with 20μg/ml proteinase K (Sigma-Aldrich, Oakville ON) for 10 min at room temperature, followed by a wash in 2 changes of PBS. Excess liquid was removed from the tissue sections by blotting and an equilibration buffer (supplied) was applied directly to the slide and incubated for 30 sec. The excess liquid was removed and the terminal deoxynucleotidyl transferase enzyme with nucleotides and a digoxigenated cytosine (supplied) was applied directly to the tissue and covered with a plastic coverslip.

The slides were incubated in a humidified chamber for 1 h at 37°C. Slides were then immersed in stop/wash buffer (supplied) for 10 min and washed with 3 changes of PBS. The excess liquid was removed and anti-digoxigenin-fluorescein (FITC) conjugate was applied to the tissue sections, covered with a plastic coverslip and incubated at room temperature in a humidified chamber for 30 min. Slides were washed in 4 changes of PBS, the excess moisture was removed and the slides were allowed to air dry. The tissue sections were counterstained with 0.4μg/ml 4',6-diamidino-2-phenylindole (DAPI), a fluorochrome that binds to double-stranded DNA, in Antifade® (Serologicals, Temecula CA) and mounted under a glass coverslip. The slides were analyzed on the Zeiss Axiophot 2 image analysis system, using a 63x oil immersion objective (total magnification: 630X). Slides were scored using a dual bandpass filter designed to simultaneously view FITC (apoptotic DNA) and DAPI (total DNA). Apoptotic nuclei were identified as positive for both the DAPI counter-stain and FITC with the dual bandpass filter. Apoptotic cells were confirmed by viewing the positive cells individually with separate FITC (ex. 490nm & em. 520nm) and DAPI (ex. 365nm & em 480nm) filters. Apoptotic positive cells were also confirmed morphologically having a nucleus that was homogenously staining and crescent shaped and overall smaller cell size.

The cell density in the brains of TGM and age-matched normal mice was scored by manually counting cell nuclei stained with DAPI. The slides were counted at a magnification of 630X to aid in the morphological identification of nuclei. Total cell numbers per field of view were counted for the entire tissue section.

SPECT and PET Imaging

Twelve male mice ages 11 − 12 months were used for imaging in four experimental groups; untreated Nr, untreated TGM, MDS-Nr, MDS-TGM ($n = 3$) Mice used for SPECT imaging were injected via tail vein with approximately 15 MBq ^{99m}Tc-HMPAO. The compound was allowed to circulate for 15 min, at which time the animals were sacrificed and imaged overnight to maximize image resolution. SPECT scans were acquired on an X-SPECT system (Gamma Medica, Northridge, CA) using dual sodium iodide crystals in combination with low energy pinhole collimators with 1 mm aperture and a radius of rotation of 3.5 cm. The SPECT scan consisted of thirty-two 15-min projections and was followed immediately by the collection of four rotations of 1024 X-ray projections for CT, also acquired on the X-SPECT system with X-ray tube characteristics of 75 kVp and 220 μA.

Mice used for PET imaging were injected with 11-14 MBq ^{18}F-FDG via the tail vein. The compound was allowed to circulate for 60 min, at which time, the animals were sacrificed and imaged overnight to maximize image resolution. PET scans were acquired on a MOSAIC small animal PET scanner (Philips, Andover MA). PET images were acquired over an 8-hr period, followed immediately by the collection of four rotations of 1024 X-ray projections for CT, acquired on the X-SPECT system. All imaging work was completed at the McMaster Centre for Preclinical and Translational Imaging (MCPTI) at McMaster University (Hamilton, ON, Canada).

Statistical Analyses

Statistical tests applied are described in corresponding figure and table captions. Briefly, where age-ranges were available, effects of treatment, genotype, gender, and other independent variables were first assessed with ANCOVA (covariate = age). If main effects or interaction effects were not resolved for a given predictor variable, groups (or ages) were pooled. Effects of the remaining variables were discriminated with post-hoc SNK or Duncan's tests. In the absence of other predictor variables, effects of treatment were resolved with a *t*-test. A two-tailed (Fisher's) chi-square test was used when comparing number of animals eliciting positive responses in each treatment group on behavioral tests of visual acuity and somatosensory function. Where applicable, age-related effects were analysed described with linear regressions.

RESULTS

Three-month-old Nr and TGM mice (Fig. 1A), illustrate the difference in adult body size in the mice. Average body masses for female Nr and TGM mice at 4 months of age were 30.1 ± 2.36 g and 46.8 ± 0.33g respectively [Lemon et al., 2003]. Twelve-month old control and MDS supplemented TGM were shown in Figure 1B to illustrate the dramatic improvement in body

Environmental and Molecular Mutagenesis. DOI 10.1002/em

TABLE I. Open Field: Effects of Age, Genotype, and Treatment on Distance Traveled by Zone, and Mean Running Velocity ($n = 56$)

Independent variable	Central zone: Distance traveled (ANCOVA)	Peripheral zone: Distance traveled (ANCOVA)	Mean running velocity (ANCOVA)
Age	***P* < 0.012**	***P* < 0.016**	***P* < 0.001**
Genotype	***P* < 0.001**	***P* < 0.001**	***P* < 0.001**
Treatment	$P > 0.118$	$P > 0.518$	$P > 0.313$
Genotype*Treatment	***P* < 0.034**	$P > 0.733$	$P > 0.792$
Difference in slopes			
Genotype*Age	$P > 0.809$	$P > 0.913$	$P > 0.777$
Treatment*Age	$P > 0.441$	$P > 0.543$	$P > 0.688$
Genotype* Treatment*Age	$P > 0.935$	$P > 0.386$	$P > 0.655$

Strong effects of age and genotype were resolved for all variables. Treatment affected distance traveled in central zone only. Slopes of age-related regressions were compared and found to be independent of either genotype, treatment, or genotype*treatment.

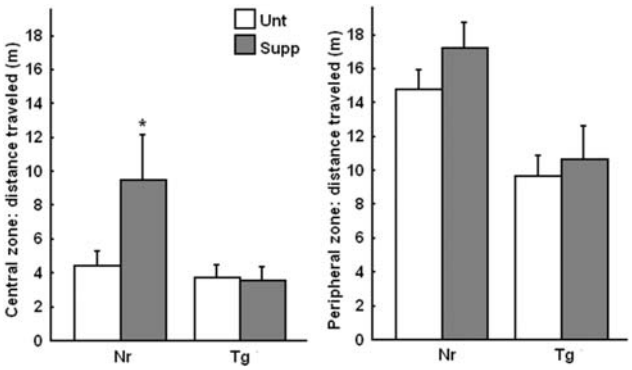

Fig. 2. Open field: Average distance traveled in central and peripheral zones by Nr untreated ($n = 14$) and MDS ($n = 10$) mice, and TGM untreated ($n = 17$) and MDS ($n = 15$) mice in a 5-min period. MDS Nr mice covered 113% ($P < 0.003$) more distance in the central zone compared to untreated Nr controls. No treatment effects in TGM mice were seen. Distance traveled in peripheral compared to central zone was greater for all groups ($P < 0.0001$). Effects of treatment on travel distance in the peripheral zone were not resolved. Combined, TGM covered a ~40% shorted distance in the peripheral zone compared to Nr mice ($P < 0.0005$).

condition of MDS supplemented TGM compared to age-matched untreated TGM (coat colour has been previously determined as an irrelevant variable).

Behavioral Analysis

Open Field

Nr and TGM mice aged between 4–18 months were scored on four parameters in a brightly illuminated open field ($n = 56$); (a) Latency to exit the central zone was not affected by age, genotype or treatment (data not shown). (b) Distance traveled in peripheral zone was affected by age and genotype but not treatment (Table I). Oldest mice (15–18 months) traveled ~15% less (data not shown), and TGM covered ~40% less distance than Nr mice (Fig. 2). Slightly greater distances traveled by supplemented mice were not significantly resolved (Fig. 2). All mice traveled greater distances in peripheral compared central zone (Fig. 2). (c) Distance traveled in central zone was reduced across age-range (~30% from 4 to 18 months; Table I). A significant effect of genotype was resolved, but this reflected a genotype*treatment interaction mainly associated with changes in Nr behavior (Table I). MDS Nr mice traveled more than double the distance covered by untreated Nr ($P < 0.003$; Fig. 2). Supplementation had no effect on distance traveled in the central zone in TGM mice (Fig. 2). (d) Mean running velocity was not affected by treatment (Table I). TGM were slower compared to Nr mice by 24% and mean running velocity was negatively correlated with age (Table I). Parameters (a–d) showed significant age-related regressions when genotypes and treatments were pooled (Table I). For each parameter, we assessed whether MDS supplemented and untreated Nr and TGM mice resolved different slopes for age-related regressions. Differences in slopes were not resolved with ANCOVA (Table I) indicating that impacts of age were similar for all groups and were unaffected by genotype or treatment.

Step-Down Test

Latency to step down from an elevated platform was first measured under bright illumination, and following a rest period, a repeat assessment was performed in near-darkness. A small number of animals used in the dark trials were different than those tested in bright illumination. Latency to step down was significantly affected by MDS treatment and level of illumination; however age and genotype did not significantly influence latency (Table II). To increase statistical power, ages and genotypes were pooled. For untreated animals, the latency to step down did not significantly differ between bright ($n = 67$) and dark ($n = 39$) illumination (Fig. 3). However, in supplemented mice differences between bright ($n = 73$) and dark ($n = 21$) illumination resulted in a significant 38% decrease in step-down latency (Fig. 3). In bright conditions, supplemented mice showed a non-significant decrease ($P > 0.151$) in latency compared to untreated controls. Latency to step down in dim illumination was significantly reduced in MDS supplemented mice ($P < 0.038$; Fig. 3).

Circle Run

Effects of age, genotype, treatment, and illumination on latency to (a) emerge from cup and (b) escape to shade are presented in Table III. The same group of mice was tested in bright and dark conditions, with one week between trials. Effects of age and genotype were not significantly resolved (Table III), to increase statistical

J_ID: z8i Customer A_ID: EM22019 Cadmus Art: EM22019 Ed. Ref. No.: EMM-15-0117.R1 Date: 29-April-16 Stage: Page: 7

TABLE II. Step-Down Test: Effects of Variables on Latency to Step Down

Independent variable	ANCOVA
Age	$P > 0.061$
Genotype	$P > 0.075$
Treatment	***P* < 0.009**
Illumination	***P* < 0.037**
Genotype*Treatment	$P > 0.972$
Genotype*Illumination	$P > 0.985$
Treatment*Illumination	$P > 0.589$

Strong effects of treatment and illumination were found. Age and genotype were marginally resolved, which allowed pooling Nr and TGM across ages. Total: $n = 141$ mice.

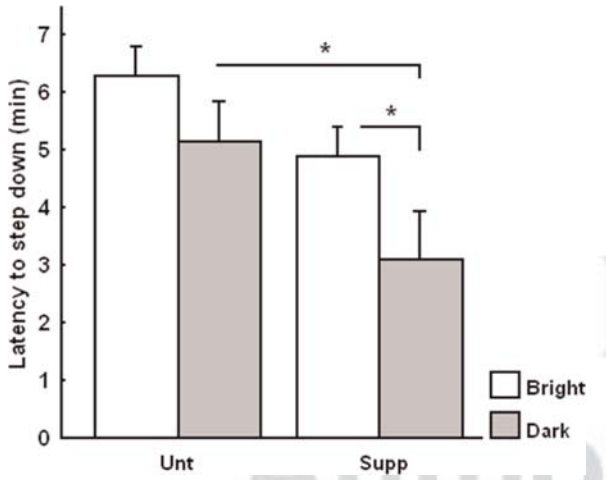

Fig. 3. Step-down test: Latency to step down was pooled across genotypes (refer: Table II). Untreated mice showed no significant differences in latency between bright ($n = 67$) and dark ($n = 39$) conditions. Supplemented mice were (38%) quicker to step down in dark illumination ($n = 21$) compared to bright illumination ($n = 73$) ($P < 0.05$). Supplemented animals were quicker to step down than controls only in dark illumination ($P < 0.038$).

TABLE III. Circle Run Test: Effects of Variables on Latency to (a) Emerge from Cup and (b) Escape to Shaded Overhang Tested with ANCOVA

Independent Variable	Latency to emerge from cup (ANCOVA)	Latency to escape to shade (ANCOVA)
Age	$P = 0.0620$	$P = 0.939$
Illumination	$P =$ **0.001**	$P = 0.096$
Genotype	$P = 0.167$	$P = 0.765$
Treatment	$P =$ **0.005**	$P = 0.532$
Illumination* Genotype	$P = 0.221$	$P = 0.055$
Illumination* Treatment	***P* < 0.001**	***P* < 0.001**
Genotype* Treatment	$P = 0.837$	$P = 0.080$

Significant effects are bolded. Combined effects of illumination*treatment were strongest for both latencies. Weak effects of age and genotype allowed for pooling of Nr and TGM data across all ages

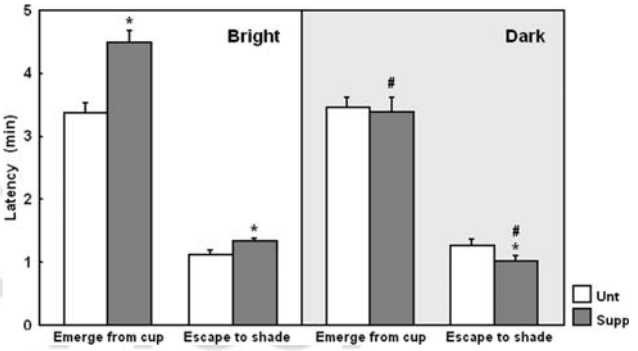

Fig. 4. Circle run test: In bright illumination both the latency to emerge from cup and the latency to reach the shaded overhang was significantly elevated in supplemented mice by 34% ($^*P < 0.0001$) and 17% ($^*P < 0.048$), respectively. Conversely, in dark conditions, latency to escape to shade was significantly lower in supplemented mice by 18% ($^*P < 0.019$) compared to untreated controls. Going from bight to dark illumination the latency to emerge from cup and to escape to shade was significantly lowered only in supplemented mice by 25% ($^{\#}P < 0.0001$) and 21% ($^{\#}P < 0.006$), respectively. Responses of untreated mice were virtually identical in either illumination.

power Nr and TGM mice were combined across ages. (a) Latency to emerge from cup. Untreated mice took the same amount of time to emerge from the cup regardless of illumination (Fig. 4). Compared to untreated mice, MDS supplemented mice took 34% longer ($P < 0.0001$) to emerge in bright illumination (Fig. 4). Alternatively, when tested in near-darkness, supplemented mice emerged from the cup significantly faster ($P < 0.0001$) than in bright lighting (Fig. 4). (b) Latency to escape to shade. Latency to escape to shade was unchanged in untreated mice regardless of level of illumination (Fig. 4). In bright conditions, MDS mice spent 17% ($P < 0.048$) longer in the open zone before entering the escape overhang compared to controls. However, when tested in dim illumination, escape time of MDS mice was 18% faster relative to controls ($P < 0.019$; Fig. 4). This result was also demonstrated in the significantly different escape latency of MDS mice going from bright to dark illumination ($P < 0.006$; Fig. 4).

Rotarod

Latency to fall off a rotating cylinder was measured on three consecutive trials. Mean (3–trial average) latency was nearly 4 times lower in TGM compared to Nr mice; but effects of treatment on mean latency were unresolved in either genotype (Fig. 5A). A key aspect of this test, however, is rate of improvement. Improvement was scored by subtracting latency to fall on the first trial from that on the last attempt. Improvement was not affected by genotype ($P > 0.390$); hence we combined Nr and TGM mice for better statistical power (Fig. 5B). Untreated mice

ID: nagarajulum Time: 13:44 I Path: //chenas03/Cenpro/ApplicationFiles/Journals/Wiley/EM##/Vol00000/160017/Comp/APPFile/JW-EM##160017

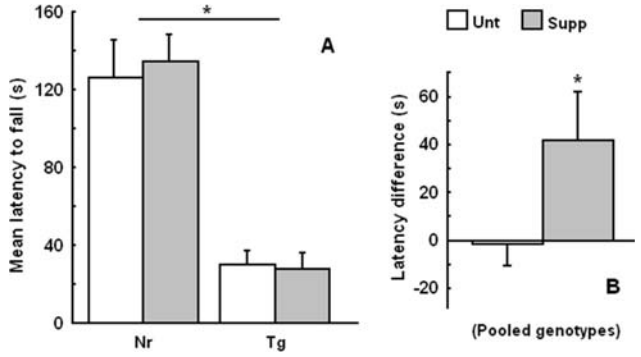

Fig. 5. Rotarod motor balance test: (**A**) Mean latency to fall (3 trial average) for untreated ($n = 12$) and supplemented Nr ($n = 9$) and untreated ($n = 17$) and supplemented TGM mice ($n = 7$). Effects of age ($P > 0.625$), body weight ($P > 0.469$) and treatment ($P > 0.759$) were not resolved. Overall TGM mice were over four times quicker to fall compared to Nr (effect of genotype: $P < 0.002$). **B**: The difference in latency to fall between the first and last trial was calculated by subtracting latency on the last trial from the latency on the first attempt. Nr and TGM mice were pooled as effects of genotype were not resolved ($P > 0.390$). Untreated mice showed no improvement on repeated attempts whereas supplemented mice had a ~40 sec improvement by the last trial ($^*P < 0.044$).

TABLE IV. Number of MDS and Untreated Nr Mice Showing Positive Responses in Crude Somatosensory Tests

Test	Mice showing positive responses Untreated Supplemented	Chi-square
Landing response	27 of 29 27 of 27	$P = 0.492$
Visual placing	34 of 37 28 of 29	$P = 0.625$
Negative geotaxis	34 of 40 39 of 42	$P = 0.307$
Pinch reflex	29 of 29 27 of 27	$P = 1.000$

MDS treatment did not improve somatosensory scores as nearly all untreated mice exhibited positive responses to all testing

showed no improvement between by the last trial, but supplemented mice improved by ~40 sec, which was significantly resolved ($P < 0.044$; Fig. 5B). This improvement corresponded to one third of the initial latency.

Simple Somatosensory Tests

Results of the (a) landing response, (b) visual placing, (c) negative geotaxis, and (d) pinch reflex are summarized for Nr (~2-year-old) mice (Table IV). Virtually all mice showed normal function in these simple somatosensory tests and further improvement from supplementation was not possible (Table IV).

Visual Acuity

A newly developed protocol was used to assess visual acuity of 1.5- to 2-year-old Nr mice. Animals were challenged with six visual cues of increasing difficulty. A reaching response indicated that mice were able to see the cue. All mice showed a reaching response on the least difficult challenge (#1; Table V). As difficulty increased (challenges: #2–5), progressively fewer mice successfully located the visual cue. The number of animals maintaining positive responses was consistently greater in the MDS group (Table V). On challenge #4, 63% of MDS mice displayed a reaching response compared to 23% in untreated mice ($P < 0.014$; Table V). A greater than 60% drop-off in reaching responses occurred for untreated mice between challenge #3 to #4.

In MDS mice, a comparable drop was observed, however it occurred between challenges #4 to #5. No mice showed reaching responses on challenge #6 (Table V) which employed nearly complete darkness, providing a negative control, confirming that responses on the easier challenges were indeed due to visual acuity.

Olfactory Sensitivity

Olfactory sensitivity was measured by quantifying the duration of exploration in response to varying concentrations of an attractive scent (peanut butter). Both supplemented and untreated mice spent little time (~130 sec) investigating filter papers with zero or low (0.125 mg/10 ml) concentrations of peanut butter. When presented with higher (0.250 mg/10 ml, and 0.500 mg/10 ml) concentrations, supplemented mice increased exploratory behavior duration by 68% and 105%, respectively. Plotting the mean duration of exploratory behavior (Y-axis) over peanut butter dilution (X-axis) for supplemented mice returned a strong positive correlation (i.e., dose response) ($r^2 = 0.976$; $P < 0.012$; Fig. 6). Conversely, untreated mice showed nearly no change (<10% increase) in exploration going from zero to high peanut butter concentrations ($r^2 = 0.069$; $P > 0.738$; Fig. 6). Slopes of regressions significantly differed for treatments (ANCOVA: $P < 0.036$).

Brain Cell Number and Weight

There is significant difference in brain cell density in 12-month-old untreated TGM (Fig. 7A) and MDS TGM (Fig. 7B). Brain cell number was determined by manually counting the number of DAPI stained nuclei in each brain slice at 630X magnification (same tissue sections as those used for the Apoptag® assay), and totalling the number of cells from all brain sections. There was no significant difference in total brain cell number between 3-month-old untreated and MDS Nr mice (94,646.7 ± 9,098.4 and 100,816.0 ± 7,944.6, respectively, $P > 0.636$; Fig. 8A). Three-month-old untreated Nr mice had 77.4% of the brain cells found in age-matched untreated TGM. Three-month old TGM also demonstrated no significant differences in brain cell number when MDS supplemented animals (118,194.7 ± 6,337.2) were compared to control

TABLE V. Results of the Visual Acuity Test in MDS and Untreated Nr Mice ($n = 22$ per group; age: 1.5–2 years)

Visual challenge	Reaching responses Untreated (%) Supp (%)	Chi-square
#1: 5mm wire, white background, room light	22 (100) 22 (100)	$P = 1.000$
#2: 5mm wire, black background, room light	20 (91) 21 (95)	$P = 1.000$
#3: 1mm wire, black background, room light	14 (63) 18 (82)	$P > 0.310$
#4: 0.5mm wire, black background, room light	5 (23) 14 (63)	$\mathbf{P < 0.014}$
#5: 0.5mm wire, black background, dim light	1 (5) 4 (18)	$P > 0.345$
#6: 0.5mm wire, black background, near-dark	0 (0) 0 (0)	$P = 1.000$

The proportion of mice exhibiting reaching responses decreased with increasing difficulty. A significant difference was resolved on a moderately difficult challenge (#4) indicating that supplemented mice had better visual acuity. All mice showed a reaching response on the easiest task (#1) and all reaching responses were completely extinguished on the most challenging task (#6). Effects of gender were not resolved

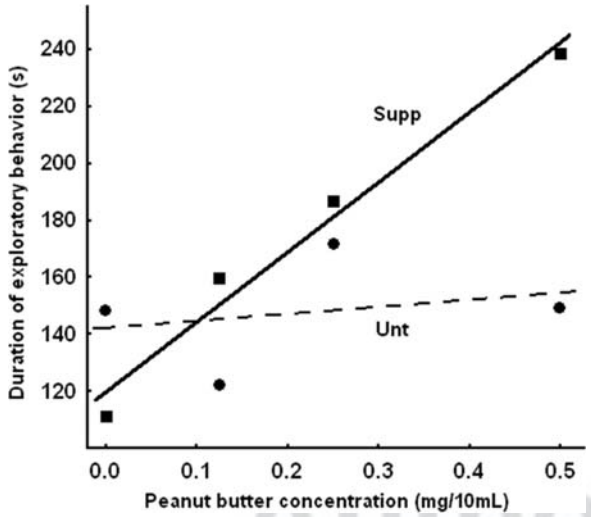

Fig. 6. Olfactory sensitivity: Relationship between duration of exploratory behavior and concentration of olfactory cue (peanut butter) for supplemented ($n = 11$) and control ($n = 11$) Nr mice (age: 1.5–2 years). Each point is the mean value of exploratory duration averaged for 11 mice in each treatment group. No significant regression was seen in untreated mice. A strong positive relationship was observed in supplemented mice indicating a dose response mechanism. Linear regressions: Untreated: $y = 142.145 + 25.101*x$; $r^2 = 0.069$; ($P > 0.738$); Supplemented: $y = 119.763 + 245.964*x$; $r^2 = 0.976$; ($P < 0.012$). ANCOVA (covariate = concentration) resolved a significant difference in slopes of regression lines between treatments ($P < 0.036$).

mice (122,358.7 ± 2,553.3; $P > 0.575$). Control and MDS 12-month-old Nr mice were not significantly different with respect to brain cell numbers with mean values of 78,545.3 ± 7,165.2 and 85,312 ± 6,013.1, respectively ($P > 0.509$). Untreated 12-month old TGM had a mean of 53,513.3 ± 2,151.9 brain cells, significantly lower than age-matched MDS TGM with mean brain cell number of 120,514.6 ± 1,570.7 ($P < 0.00001$). 12-month old MDS TGM did not differ significantly in brain cell number from either 3-month-old untreated or MDS supplemented TGM ($P > 0.740$ and $P > 0.571$, respectively). Analysis of variance (ANOVA) detected a significant impact of genotype on mean brain weight ($P < 0.000001$), no other significant main effect was detected for any other variable. ANOVA did reveal a strong interactive effect between genotype and supplement ($P < 0.06$) and between genotype and age ($P < 0.05$), with only the latter reaching significance. Analysis of mouse brain weight (Fig. 8B) demonstrates that 3-month-old Nr mouse brains were only 57.3% (483 ± 34 mg) of the mass of young TGM controls (843 ± 79 mg; $P < 0.0100$). Three-month old supplemented Nr (487 ± 40 mg) and supplemented TGM (851 ± 47 mg) do not differ from their controls in brain weight ($P < 0.942$ and $P < 0.934$, respectively).

Three-month old control TGM had significantly greater brain mass than 12-month-old control TGM at 541 ± 67mg ($P < 0.011$) and 12-month-old Nr mice at 534 ± 73 mg ($P < 0.013$). Twelve-month old control TGM brain mass was 64.2% of young control TGM brains. Twelve-month old control TGM did not differ significantly in brain weight from either age-matched control Nr ($P > 0.949$) or 3-month old control Nr mice ($P > 0.590$). The brain weight of 12-month-old supplemented TGM (873 ± 51 mg) was significantly greater than 12-month-old control TGM ($P < 0.003$), but did not differ significantly from 3-month-old control TGM ($P > 0.770$) or supplemented TGM ($P > 0.763$). Twelve-month-old supplemented Nr mice (522 ± 38 mg) did not differ from age-matched control Nr mice in brain weight ($P > 0.896$).

Apoptosis

Apoptotic cells were identified with Apoptag®, a modified TUNEL assay, used to detect fragmented DNA associated with apoptotic nuclei. Since the entirety of each brain slice was scored for apoptotic cells, the total number of cells scored varied for each experimental group (Fig. 8C), apoptotic cells are identified as a percentage of the total number of cells in the brain slices. The results from all groups (3-month-old and 12-month old, control and supplemented) showed that only 3-month-old control Nr mice had an elevated level of apoptosis ($P < 0.05$; Fig. 8C). Although the level of apoptosis in young Nr controls is significantly elevated compared to all other groups it was still below 0.1%, so the biological significance of this finding is undetermined.

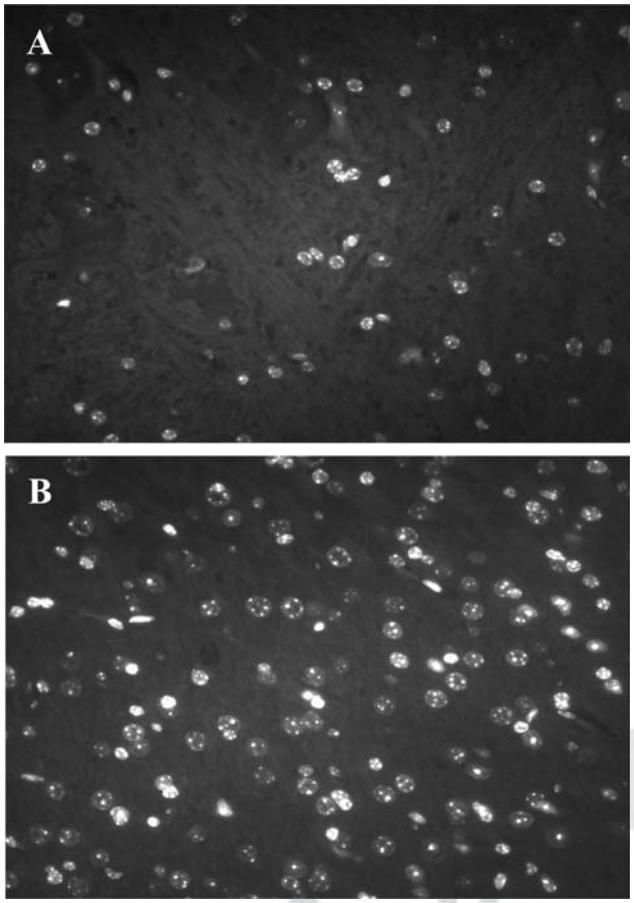

Fig. 7. Brain sections with DAPI stained nuclei at 630x magnification. (**A**) 12-month-old control TGM (**B**) 12-month-old supplemented TGM. The most acellular region was in an area encompassing the bed nuclei of the stria terminalis and reticular nucleus of the thalamus (Lateral 0.675 mm; Bregma −0.25mm to −0.65mm, and 4.00 mm to 4.50 mm).

Tissue Morphology

Cerebellum Histology

Purkinje cells (PC) in inter-hemispheric sagittal cerebellar sections of lobules II and III (Fig. 9A) were counted in Nr mice aged 14–17 months (narrow age-range precluded analysis of age-related trends; supplemented: n = 6; untreated: n = 6). PC are restricted to the Purkinje cell layer (Figure 9B) and length of the Purkinje cell line were accounted for when counting cells [Rogers et al., 1984; Woodruff-Pak, 2006]. Supplemented mice showed a 20% increase in PC number per mm of cell line ($P < 0.05$; Fig. 10A). Figure 9D shows a close up of PC from supplemented and untreated mice dyed with Nissl stain. PC in a sample from an untreated mouse show visibly reduced PC number compared to supplemented mice. Average thickness of the molecular layer (ML) and granular layer (GL) in Lobules II and III were calculated using ImageJ software according to schematic shown in Figure 10C. Supplemented mice had a 16% ($P < 0.05$; Fig. 10B) and 18% ($P < 0.01$; Fig. 10C) increase in thickness of the ML and GL, respectively, compared to untreated mice. Cerebella were collected from three male and three female mice in each treatment group. An effect of gender or gender*treatment interactive effects were not resolved.

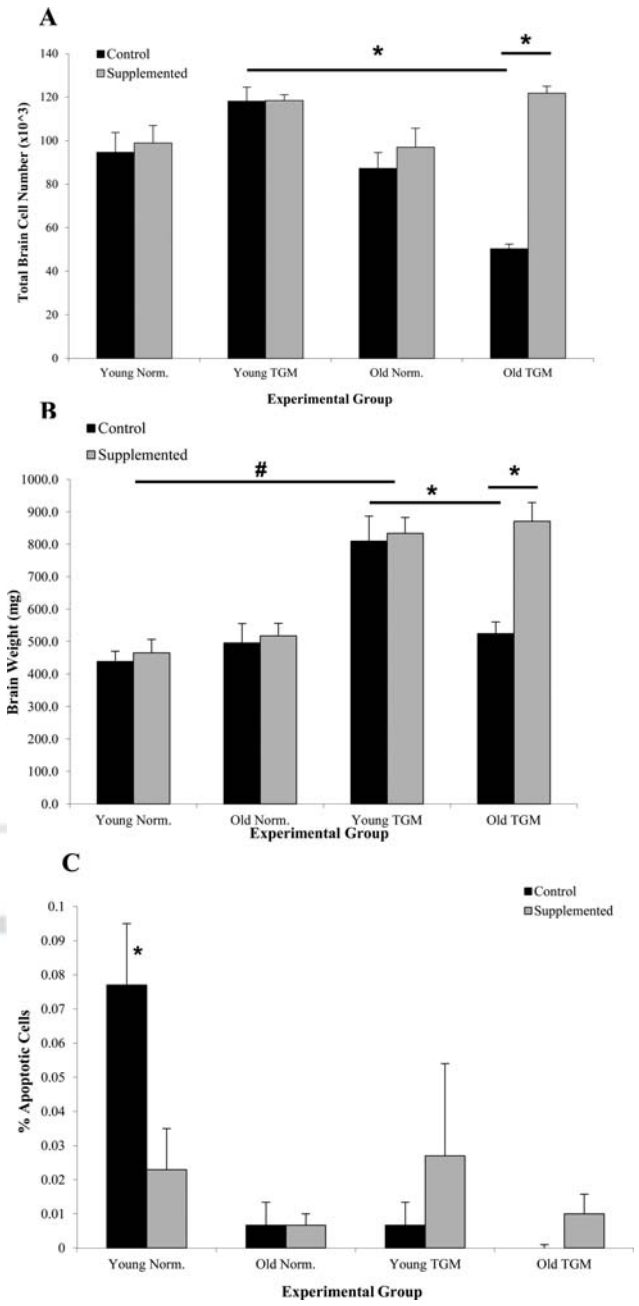

Fig. 8. Markers of brain deterioration in untreated TGM mice relative to normal mice and MDS supplemented TGM. **A**: Total number of DAPI stained brain cell nuclei from 4 brain slices (* $-P < 0.00001$). **B**: Brain weight for 3-month-old and 12-month-old mice, either control or diet supplemented. Weight represents wet mass of brain taken immediately after dissection (# $-P < 0.01$; *$-P < 0.013$). **C**: Percentage of apoptotic cells calculated from the total number of cells in 4 sequential brain slices. Mean ± standard error are given for each group (*$-P < 0.05$).

J_ID: z8i Customer A_ID: EM22019 Cadmus Art: EM22019 Ed. Ref. No.: EMM-15-0117.R1 Date: 29-April-16 Stage: Page: 11

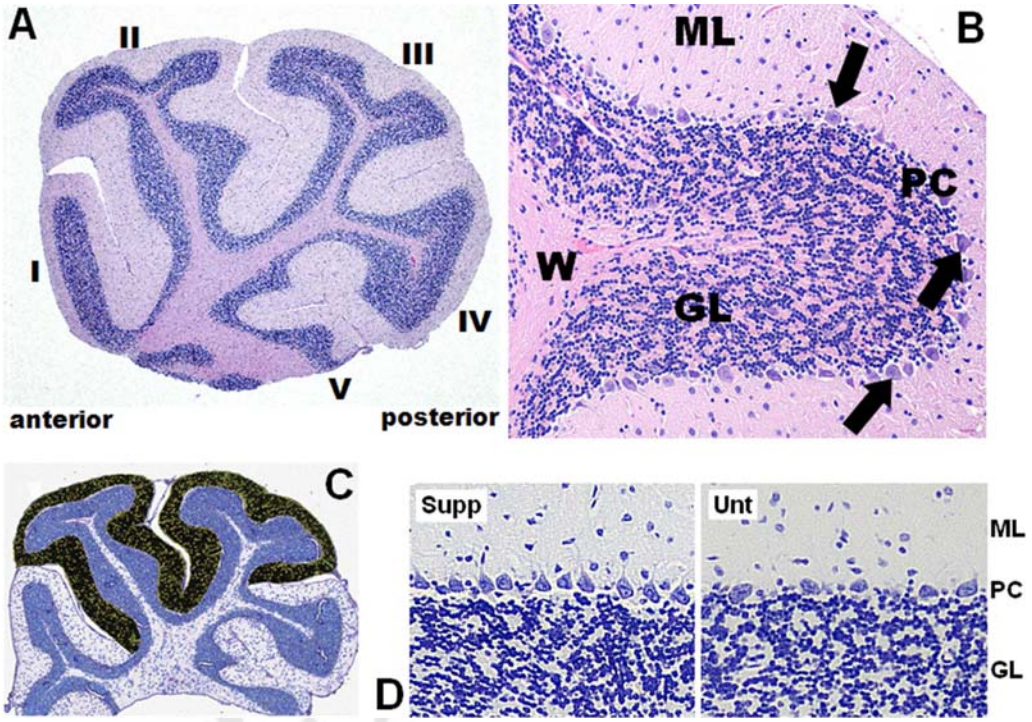

COLOR

Fig. 9. **A**: Macrostructure of the mouse cerebellum: Interhemispheric sagittal cerebellar section showing lobules I–V (H&E, ×40 magnification). Purkinje cells were counted in Lobules II and III. **B**: Microstructure of the cerebellum: Showing molecular layer, ML; white matter, W; granule cell layer, GL; and Purkinje cell layer, PC. Arrows point to individual Purkinje cells which are organized in a single layer on the border of ML and GL (H&E, ×100 magnification). **C**: Image processed using ImageJ software. Dark area shows the section of ML used to calculate mean ML thickness. Portion of the GL underlying the dark region was used to calculate mean GL thickness. **D**: Representative slides from matching cerebellar areas of supplemented and untreated mice (NISSL stain, ×100 magnification). Notice the relative scarcity of Purkinje cells in untreated tissue compared to supplemented. All tissue sectioned at 5 μm.

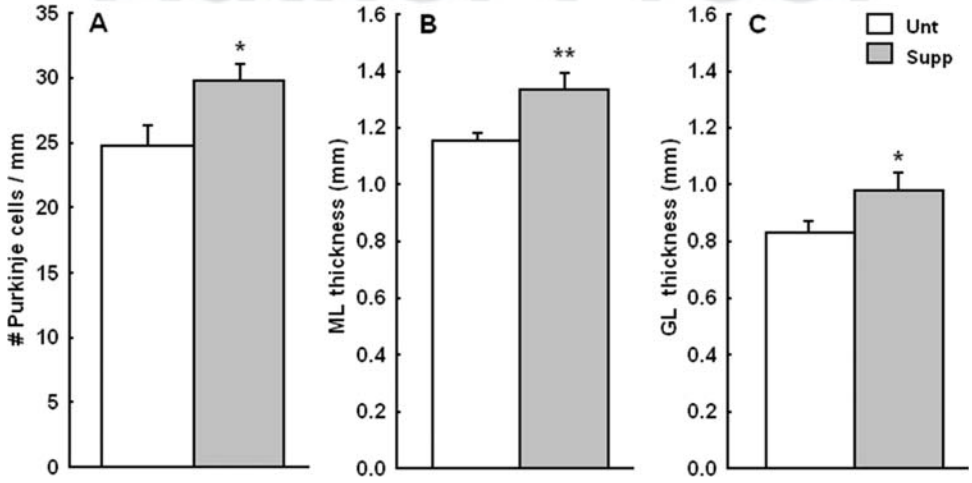

Fig. 10. **A**: Number of Purkinje cells per mm of cell line length in cerebella of Nr mice. Supplemented mice had 20% more Purkinje cells compared to controls (*$P < 0.05$). **B**: Average thickness of ML and (**C**) GL in cerebellar Lobules II and III. Thickness of ML and GL was greater in supplemented mice by 16 and 18%, respectively, compared to untreated control (*$P < 0.05$, **$P < 0.01$). Effects of sex were not resolved, $n = 6$ mice per group, age: 14–17 months.

Retina Histology

Mid-sagittal sections of eyes were stained with H&E in supplemented ($n = 4$) and untreated ($n = 4$) 2-year-old Nr females (Fig. 11A). In supplemented mice, thickness of ONL and OS averaged over the length of proximal retinal sections (Fig. 11) were 26% and 29% greater, respectively, compared to controls (Fig. 12). Close-ups of

Environmental and Molecular Mutagenesis. DOI 10.1002/em

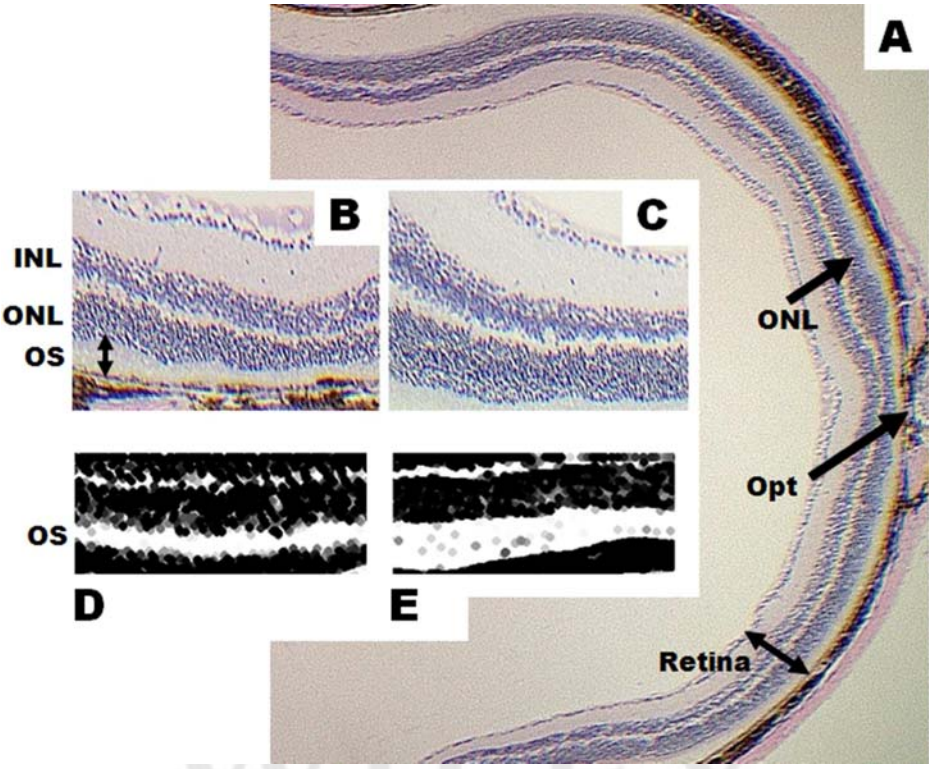

COLOR

Fig. 11. **A**: Sagittal cross-section of the eye showing retinal organization (×40 magnification). **B,C**: Enlarged sections of proximal retina from an untreated and supplemented mouse (×100 magnification) showing the inner nuclear layer, INL; outer nuclear layer, ONL; and outer segments, OS. Notice the visible reduction in ONL thickness from an untreated mouse (B) compared with supplemented (C). **D,E**: Images processed with ImageJ software digitally isolating the OS (white) from surrounding layers (black). Average thickness of OS was calculated by digitally computing the "white" area and dividing by the length of the layer. Notice the visibly reduced OS in an untreated (D) compared with a supplemented (E) mouse. ONL and OS were measured along the proximal retinal portion which was set at 1,000 μm superior and inferior to position of optic nerve attachment, Opt. Sections were cut at 5 μm and stained with H&E.

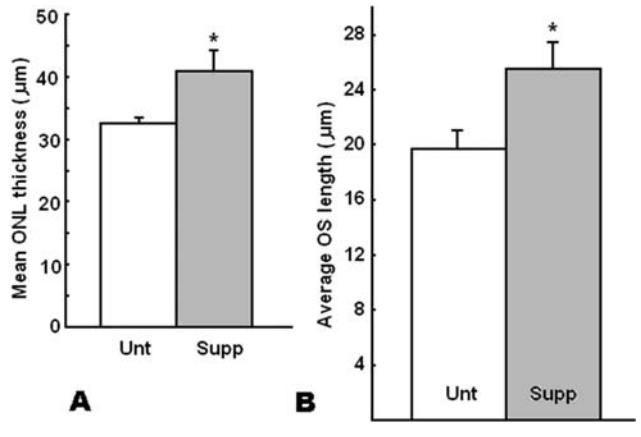

Fig. 12. Average ONL (**A**) and OS (**B**) thickness in proximal retinal regions of supplemented and untreated Nr mice ($n = 4$ per group; age ~2 year). Mean ONL thickness was 32.71 ± 2.44 μm and 41.14 ± 2.44 μm for untreated and supplemented mice, respectively (26% difference; $^*P < 0.05$). Mean OS thickness was 29% greater in supplemented mice (25.65 ± 1.87 μm) than in untreated controls (19.81 ± 1.21 μm) ($^*P < 0.05$).

retinal sections from supplemented and control mice showed visible differences (Figs. 11B–11E).

Olfactory Bulb Histology

Cross-sections of olfactory bulbs were obtained from supplemented ($n = 6$) and untreated ($n = 5$) mice (ages: 14–17 months). ImageJ was used to calculate mean thickness of glomerular layer (GLM) and external plexiform layer (EPL) (organization of neuronal layers shown in: Fig. 13A). GLM and EPL were significantly reduced in supplemented mice by 25% ($P < 0.026$; Fig. 14B) and 28% ($P < 0.001$; Fig. 14C) respectively, compared to controls. F14

Mitral Cell Layer

For counts of mitral cells strict criteria were applied including cell size, shape, position, and visibility of clearly defined nuclear envelope and nucleolus (Figs. 13B and 13C). Although this underestimates total cell numbers it provides maximal accuracy for comparisons between samples. Mitral cell counts in a 1 mm representative section were 29% higher in supplemented mice compared to controls ($P < 0.030$; Fig. 14A). Despite this significant

J_ID: z8i Customer A_ID: EM22019 Cadmus Art: EM22019 Ed. Ref. No.: EMM-15-0117.R1 Date: 29-April-16 Stage: Page: 13

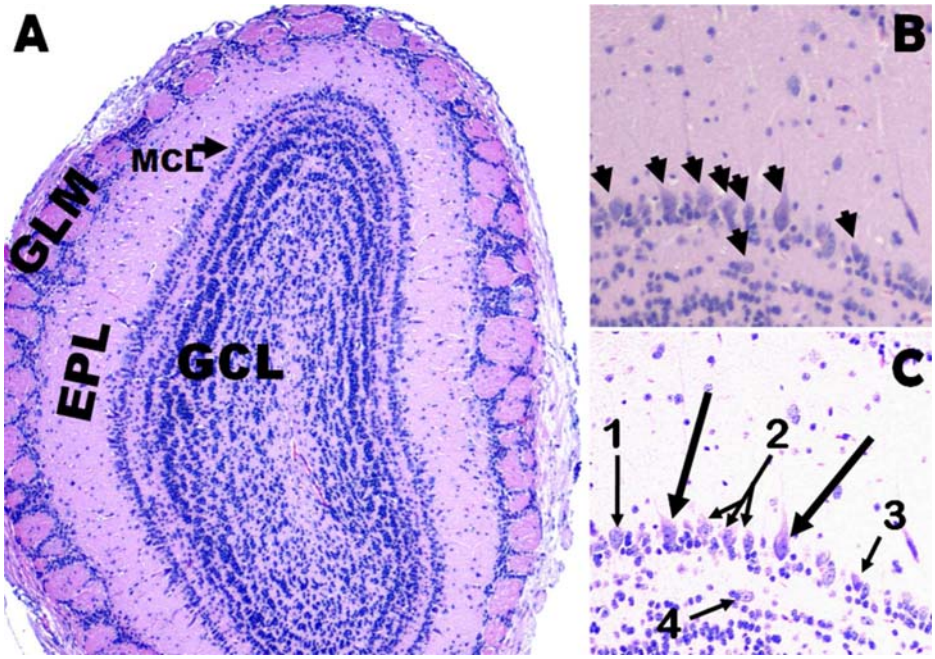

COLOR

Fig. 13. **A**: Cross section of mouse olfactory bulb showing the glomerular layer, GLM; external plexiform layer, EPL; mitral cell layer, MCL; and granule cell layer, GCL (×40 magnification). **B**: Close up of the MCL (×100 magnification) showing several pyramidal-shaped mitral cells. Granule cells occur in the MCL but appear smaller and darker than mitral cells. Arrow heads point to probable mitral cells, but accurate classification is difficult as cells show a range of sizes, variable spatial orientation, overlapping, and may occur outside the MCL. For maximal consistency, careful discrimination criteria were applied: **C**: Image processed with ImageJ software to highlight cellular structure. Only cells greater than five pixels across were counted (cell 3 does meet size criteria). Only cells with clearly defined nuclear envelope and nucleolus were counted (large arrows). Cells 1 and 2 do not clearly show the nucleus (not counted). Cell 4 is outside the MCL, hence not counted. Tissue stained with H&E, sections: 5 μm.

resolution, greater samples numbers, more representative sections and additional staining techniques could reinforce these preliminary findings.

Functional Brain Imaging

^{18}F-FDG uptake correlates to glucose utilization, which provided an indicator of brain metabolic rate (Fig. 16A). Unsupplemented 12-month-old TGM showed a significant reduction in metabolic rate compared to age-matched Nr mice ($P < 0.027$; Fig. 16A). Supplemented TGM had significantly higher brain metabolic activity than untreated TGM ($P < 0.013$; Fig. 16A), which did not differ from control or supplemented Nr mice ($P > 0.087$ and $P > 0.0.385$, respectively; Fig. 16A). Dietary supplementation had little effect on the brain metabolic rate of 12-month-old Nr mice ($P > 0.210$; Fig. 16A).

^{99m}Tc-HMPAO binds to neutrophils in the peripheral blood, providing a biomarker of blood perfusion through tissue and an important indicator of general brain function. Normal mice did not differ in brain perfusion between treatments ($P > 0.454$; Fig. 16B), however, both groups had significantly higher activity compared to unsupplemented 12-month-old TGM ($P < 0.047$ and $P < 0.023$, respectively; Fig. 16B). Untreated TGM had significantly reduced blood perfusion compared to all groups. The most striking difference was in supplemented TGM with a 2-fold increase in perfusion compared to untreated TGM ($P < 0.034$; Fig. 16B).

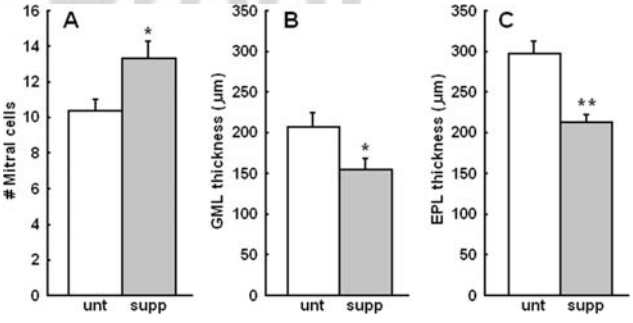

Fig. 14. **A**: Number of mitral cells meeting count criteria (Fig. 13 caption) in a 1mm representative section of mitral cell layer in olfactory bulb. Supplemented mice showed a 29% increase in cell number compared to controls (*$P < 0.030$). (**B**) Mean GLM and (**C**) EPL thickness in olfactory bulb. Supplemented mice had a 25% (*$P < 0.026$) and 28% (**$P < 0.001$) reduced GML and EPL thickness, respectively, compared to controls. Mice aged 14–17 months (untreated $n = 5$; supplemented $n = 6$).

DISCUSSION

Overall Brain Function

It has been established that TGM experience significant oxidative stress and inflammatory processes that result in

COLOR

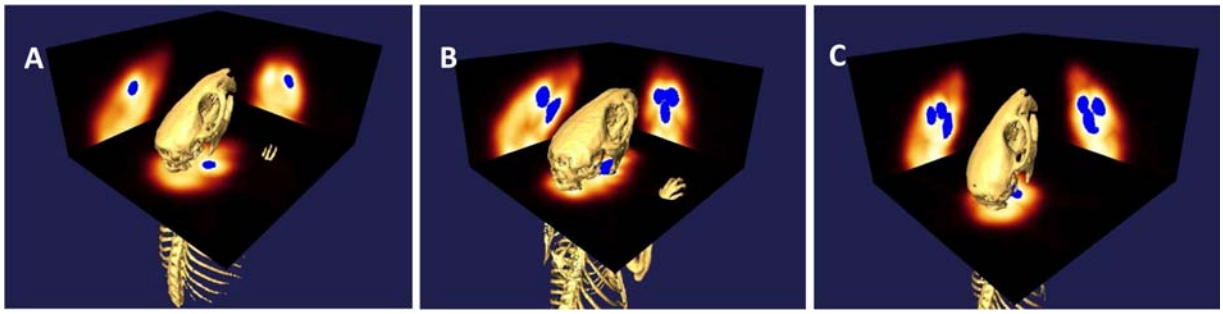

Fig. 15. Levels of ^{18}F-FDG uptake in the brains of 12-month-old mice. **A**: Unsupplemented TGM. **B**: Unsupplemented normal mouse. **C**: Supplemented TGM. Activity normalized to uptake in skeletal muscle.

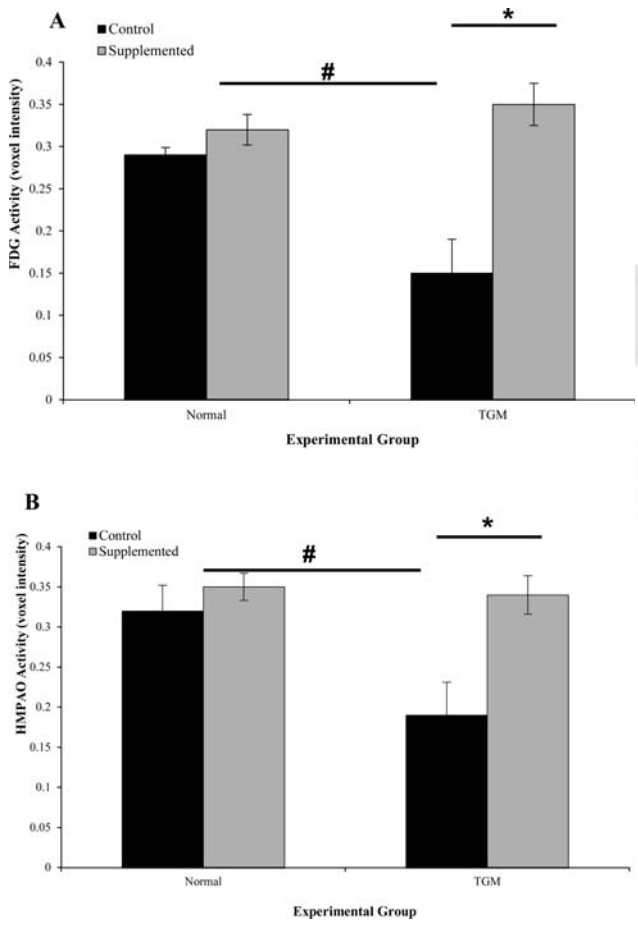

Fig. 16. Brain uptake of (**A**) ^{18}F-FDG to determine brain metabolic rate (* $-P < 0.013$; # $-P < 0.027$), and (**B**) ^{99m}Tc-HMPAO to determine brain blood perfusion in control and MDS supplemented normal and TGM mice (* $-P < 0.034$; # $-P < 0.047$). Brain activity was normalized to region of low uptake (skeletal muscle) to compensate for any inter-mouse variability. Values represent mean ± SEM for each group ($n = 3$).

an accelerated aging phenotype, with dramatic negative consequences on cognitive and motor function [Rollo et al., 1996, Lemon et al., 2003, 2005, Aksenov et al., 2010, 2013, Long et al., 2012]. Severe cognitive decline was abolished by the MDS supplement formulated to target key physiological mechanisms associated with aging [Lemon et al., 2003, 2005, Aksenov et al., 2010, 2013, Long et al., 2012]. Here we show that there is a concomitant loss in brain cells, deterioration in sensory function and reductions in cerebral metabolic rate and blood perfusion in old TGM. Together these strongly contribute to age-related cognitive impairment. Brain deterioration was equivalent to advanced Alzheimer's disease in humans, with >50% losses on a cellular level, 36% loss in brain mass and at least 2-fold reductions in metabolism and blood flow. Not only did the MDS restore cognitive function in old TGM, but brain cell density and brain mass were maintained at levels comparable to young mice. To our knowledge, this is the first dietary supplement to abolish such severe loss of brain cells and maintain cognitive function with such efficacy. The mechanisms yielding such benefits are not fully elucidated; however previous research has verified MDS efficacy on improvements in all targeted mechanisms [Lemon et al., 2003, 2005; Aksenov et al., 2010, 2013; Long et al., 2012].

The complete amelioration of brain cell loss in supplemented old TGM suggests that the mechanisms targeted by the supplement (reactive oxygen species, inflammation, maintenance of cell membranes, insulin sensitivity, and mitochondrial function) were well chosen. Long et al. [2012] added nitrosative stress as another factor modulated by the MDS which is also highlighted as a factor in neurodegeneration [Nakamura and Lipton, 2007; Maurya et al., 2016]. Notably, one of the most acellular regions found in the brains of old TGM corresponds to a region (Lateral 0.675mm; Bregma −0.25 mm to −0.65 mm, and 4.00 mm−4.50 mm) encompassing the bed nuclei of the stria terminalis (BST) and reticular nucleus of the thalamus (RT). Activity within the BST correlates with anxiety in response to threat monitoring, acting as a relay site to regulate hypothalamic-pituitary-adrenal axis activity in response to acute stress [Choi et al., 2007]. The RT nucleus receives input from the cerebral cortex and dorsal thalamic nuclei. Most input comes from collaterals of fibers passing through the thalamic reticular nucleus.

Primary thalamic reticular nucleus efferent fibers project to dorsal thalamic nuclei, modulating information from other thalamic nuclei, playing a role in disinhibition of thalamic cells, an essential function for initiation of movement [Beierlein, 2014; Mitchel, 2015]. Protection of these brain regions may provide clues to the anxiolytic effect and improved motor function of MDS treated aging animals. Additionally, the apparent heterogeneity of cell loss indicates that there may be differential losses among brain regions and neurotransmitter systems in TGM, however further study will be required to confirm.

Untreated young normal mice had significantly higher brain cell apoptosis, compared to other experimental groups, although their average apoptosis was less than 0.1%. Apoptosis is a normal part of brain development which continues for several months after birth in mice. One mechanism of obtaining larger brains in IGF-1 mice is reduced apoptosis [Popkin et al., 2004], this could also apply to TGM. Old unsupplemented normal mice do not experience significant brain cell loss. A lack of significant apoptosis in old non-supplemented TGM brains was unexpected, given the chronically elevated endogenous production of ROS characteristic of TGM, and the vulnerability of the brain to oxidative damage, however it is possible that the most susceptible cells had already been lost at the advanced age of the mice used in this study. Alternatively, cells may have deteriorated rapidly via necrosis. All groups expressed very low levels of apoptotic cells, but these samples represent a single moment in time, low numbers of cell loss at constant rates still have large impacts across normal developmental and aging time scales. Brain cells from young animals are also more resistant to oxidative stress and excitotoxicity compared to adult animals [Ikeyama et al., 2002, Savory et al., 1999]. When exposed to glutamate, mitochondria in the brain slices of adult rats showed greater changes in ATP/ADP ratio, NAD/NADH ratio and ROS formation compared to young rats [Kannurpatti et al., 2004]. The 'Old' normal mice in our study were age-matched to TGM, but were middle-aged, based on average life-span of a normal mouse in our breeding colony. Consequently it would be unlikely that they would show increased brain apoptosis or significant changes brain weight or cell number. Interestingly there were non-significant increases in both metabolic rate and blood perfusion, which may indicate beneficial effects of the supplement in normal mice that could be resolved given a larger sample size. Examining the brains from senescent Nr mice in both treatment groups demonstrated that the supplement provides similar protective effects for normal aging brain [Aksenov et al., 2010, 2013]. There are a few probable explanations for the extremely low cell numbers and the apparent lack of apoptosis in old control TGM. Apoptotic cell loss is likely a significant process in untreated TGM, but if occurring at a slightly elevated homeostatic rate, would contribute to minimal differences at any one time point, but causing significant quantities of cell loss over the lifetime of the animal, with the concomitant possibility of accelerated cell loss as the animal approaches senescence. Alternatively, and less likely, there could have been a short term, large apoptotic event during middle age, when enough oxidative damage had accumulated in the brain to trigger the apoptotic response. This event may coincide with the age-related escalation in the cognitive decline observed in control TGM starting at 7 months of age [Lemon et al., 2003; Aksenov et al., 2013]. Sampling TGM brains late in senescence may have been too late to observe the mechanisms of cell loss. By 12 months of age, control TGM had only 44% of brain cells remaining compared to old diet supplemented TGM and young TGM (both control and supplemented). Harvesting brains of non-supplemented TGM at across the age spectrum may clarify the mechanism and rate of cell loss. Additional analysis on the brain tissue has provided some clarity in the mechanisms behind the profound protective effect of this dietary supplement [Aksenov et al., 2010, 2013]; however further studies will determine if there is differential cell loss in the populations of cells that comprise the brain. It will also be important to determine if specific neurotransmitter pathways are differentially affected by the substantial cell loss in control TGM.

Motor Coordination

Aging impacts motor behavior and coordinated control of motor function (i.e., balance) [Wallace et al., 1980; Foster et al., 1996; Bickford et al., 1999; Aksenov et al., 2010]. When motor coordination was tested, 12-month old untreated TGM mice had severely compromised motor coordination compared to age-matched untreated Nr, consistent with previous reports [Long et al., 2012]. Initial balance performance of Nr mice on the rotarod was not affected by MDS treatment; however MDS supplemented animals showed significant improvement in performance after three trials. Untreated Nr mice did not demonstrate such improvements, suggesting there may be a learned component to the motor coordination testing from which the MDS mice were able to benefit.

Reductions in locomotor abilities are closely linked to oxidative stress [Foster et al., 1996; Aksenov et al., 2010] and may reflect reduced mitochondrial activity [Aksenov et al., 2010]. Motor coordination has been negatively correlated with increasing levels of protein carbonyls in motor control regions of the brain including the cerebellum [Foster et al., 1996; Bickford et al., 1999]. MDS treatment significantly reduced protein carbonyls in brains of aging mice and was associated with improved locomotor behavior in MDS supplemented Nr and TGM [Aksenov et al., 2010]. Brain mitochondrial and neurotransmitter functions were also augmented [Aksenov et al., 2010, 2013], with

Environmental and Molecular Mutagenesis. DOI 10.1002/em

this study indicating that positive impacts of MDS on brain physiology manifest in better motor coordination.

While the cerebellum does not initiate movement, it is critically responsible for control, coordination and correction of body movement including sensory analysis of consequences of movement [Paulin 1993]. Animals with cerebellar defects show impaired motor coordination [Kashiwabuchi et al., 1995, Colucci-Guyon et al., 1999; Barski et al., 2003; Weimer et al., 2009]. The cerebellum has also been highlighted in motor and spatial learning [Dahhaoui et al., 1992, Le Marec et al., 1997, Bickford et al., 1999, Ito 2000, Wulff et al., 2009]. Purkinje cells (PC) are the dominant neurons involved in cerebellar information processing [Rogers et al., 1984]. They are one of the largest neurons in the mammalian brain with very intricate dendritic projections and great numbers of dendritic spines. PC provide the sole output pathway of the cerebellar cortex [Barski et al., 2000; Ito 2000] and participate in motor coordination [Barski et al., 2000, 2003] and motor learning [Bickford et al., 1999, Ito 2000, Woodruff-Pak 2006, Barski et al., 2000, Wulff et al., 2009]. Loss of PC can result in impairment of coordinated movement [Kashiwabuchi et al., 1995, Sakaguchi et al., 1996, Barski et al., 2003, Weimer et al., 2009], decreased cerebellum-dependent learning, sensory processing and other cerebellum-associated behaviors [Barski et al., 2003; Woodruff-Pak 2006, 2010]. PC are highly vulnerable neurons [Woodruff-Pak 2006] and show significant decreases in normal aging in humans and rodents [Rogers et al., 1984; Doulazmi et al., 1999; Larsen et al., 2000; Andersen et al., 2003; Woodruff-Pak 2006]. The cerebellum has been shown to express markers of senescence earlier than other brain regions, with loss or dysfunction of PC identified as a primary contributor to this phenomenon [Woodruff-Pak, 2010].

Beyond the role of the cerebellum in motor coordination, spatial processing and motor learning [Dahhaoui et al., 1992; Paulin, 1993; Kashiwabuchi et al., 1995; Sakaguchi et al., 1996; Bickford et al., 1999; Colucci-Guyon et al., 1999; Ito, 2000; Barski et al., 2000, 2003; Woodruff, 2006; Weimer et al., 2009; Wulff et al., 2009; Woodruff et al., 2010], this brain region is also implicated in perception of time [Monfort et al., 1998], autonomic functions [Tong et al., 1993; Ghelarducci et al., 1996] and emotional behavior [Bobee et al., 2000; Schmahmann and Caplan, 2006; Balaban, 2002; Schutter and Van Honk, 2005]. Several reports have documented co-morbidity of emotional and balance disorders [Balaban, 2002; Balaban et al., 2011]. In recent years, the role of the cerebellum in modulation of anxiety has been highlighted [Bobee et al., 2000; Balaban, 2002; Schutter and Van Honk, 2005; Schmahmann and Caplan, 2006; Secchetti et al., 2009], prompted largely by the discovery neuronal connections between the cerebellum and other regions of the brain involved in emotional control [Bobee et al., 2000; Balaban, 2002; Balaban et al., 2011]. Reported decades ago, abnormal cerebellar development or degeneration of cerebellar neurons produced nervous or anxious phenotypes in rodents [Sidman and Green, 1970; Landis, 1973]. To a large degree, this was attributed to loss or dysfunction of PC [Sidman and Green, 1970; Landis, 1973]. Attenuation of age-related PC loss in supplemented mice suggests that neurons involved in modulation of anxiety-related behaviors should also be intact. This is presently supported by behavioral testing and may constitute an additional anxiolytic mechanism of the MDS.

Granule cells are the smallest and most numerous neurons in the mammalian brain [D'Angelo and De Zeeuw, 2009], but relatively little is known about their specific roles. Granule cells and their synapses possess nonlinear transmission properties and are connected to allow them to operate complex transformations of input signals in the spatiotemporal domain including forms of long-term potentiation and depression. These characteristics may provide a significant impact on cerebellar learning abilities and computational power (D'Angelo 2011). Genetic mutations affecting granule cell development are associated with poor cognitive function and motor coordination [Schiffmann et al., 1999; Weimer et al., 2009]. However, isolating the effects of granule cell depletion is problematic as this is usually coupled with loss of neighboring neurons (e.g. Purkinje cells) [Le Marec et al., 1997; Schiffmann et al., 1999; Weimer et al., 2009], which can confound results. A recently proposed hypothesis argues that cerebellar granule cells compute stimuli from adjacent neurons to generate operational time-windows which set a temporal framework for integrating sensory information with motor domains [D'Angelo and De Zeeuw 2009]. This may also set the tone for long-term potentiation (LTP), effecting learning capacities. Thickness (or volume) of the granule cell layer (GL) reflects the number of granule cells [Larsen et al., 2000, Weimer et al.]. Granule cells send parallel fibers extending to the molecular layer (ML) where they interact with the dendritic arbors of Purkinje cells (PC) [Apps and Garwicz, 2005]. The ML also contains interneurons (stellate and basket cells) that provide GABAergic input to PC [Apps and Garwicz, 2005]. The ML interneurons play a role in sensory information processing and motor coordination [Apps and Garwicz 2005, Chu et al., 2012]. Aging rats lost 60% of the parallel fiber length and up to 80% of PC synapses [Huang et al., 1999], reflected by a 30% reduction of ML thickness [Huang et al., 1999]. MDS supplementation resulted in significantly increased thickness of the GL and ML, and greater numbers of PC in older mice, suggesting multiple positive benefits on cerebellar morphology. Improved motor coordination and enhanced spatial learning in older MDS supplemented mice appear

J_ID: z8i Customer A_ID: EM22019 Cadmus Art: EM22019 Ed. Ref. No.: EMM-15-0117.R1 Date: 29-April-16 Stage: Page: 17

to be a consequence of the maintenance of a more youthful cerebellar morphology.

Emotionality

Variants of the open field test have been used to assess emotionality in rodents [Trullas and Skolnick, 1993, Belzung and Griebel, 2001, Voikar et al., 2001; Carola et al., 2002; De Oliveira et al., 2007; Chaudhry et al., 2008]. However, depending on protocol variations and parameters scored, results may be more indicative of exploratory behavior than anxiety-driven responses [Trullas and Skolnick, 1993; Carola et al., 2002; Berry et al., 2007]. Variables measured in tests for anxiety (e.g. open field, elevated maze) were more consistent with general activity levels when carried out in dim light when mice are normally active [Trullas and Skolnick, 1993]. To assess emotionality we employed bright illumination and white Plexiglas construction creating aversive environments [Chaudhry et al., 2008]. Collectively, the tests performed in the current study suggest that the MDS reduced anxiety in mice, allowing supplemented mice to more freely explore an 'unsafe/novel' environment. Although the MDS was not intentionally designed to target emotionality, current findings suggest it demonstrated significant anxiolytic properties.

Essentially all variants of behavioral tests rely on movement of animals to infer emotionality levels [Trullas and Skolnick, 1993, Carola et al., 2002; Chaudhry et al., 2008]. Intrinsic differences in activity levels between treatment groups (if present) may bias interpretation. The MDS was previously shown to augment physical activity [Aksenov et al., 2010]. This could influence movement of animals in the experimental apparatus irrespective of emotionality. However, in the open field test, distance traveled by mice in the peripheral zone and mean running velocity were unaffected by MDS treatment. This indicates that increased exploration of the central zone by supplemented Nr mice was not a consequence of upregulated motor activity. In the circle run test, increased physical activity of supplemented mice would predict faster escape; however, the opposite result was observed, suggesting differences in intrinsic activity levels between treatment groups did not confound results.

Aging alone is not a significant risk factor for emotional and anxiety disorders in humans [Beekman et al., 1998]; however, some mechanisms associated with emotionality involve pathways implicated in aging. Oxidative stress has been linked to elevated anxiety in aging rodents [Berry et al., 2007; Salim et al., 2010] and reactive oxygen species (ROS) in brain positively correlate with anxiety behavior [De Oliveira et al., 2007; Bouayed et al., 2009]. Both ROS and inflammatory processes are strongly implicated in aging and age-related diseases [Finkel and Holbrook, 2000; Chung et al., Nemat et al., 2009]. Furthermore, ROS and inflammation appear to be costimulatory [Janssen et al., 1993; Lavarosky et al., 2000; Droge, 2001; Reuter et al., 2010]. Elevated ROS via NADPH oxidase activity induced anxiety which was reversed by apocynin, a NADPH oxidase inhibitor [Masood et al., 2008]. In addition, chronic inflammation and inflammatory cytokines have been shown to induce anxiety in mice and rats [Bercik et al., 2010; Song et al., 2003]. There are multiple mechanisms linking ROS and cytokines to modulation of anxiety. Neuronal losses in stress-regulating regions of the brain, altered neurotransmitter levels and dysregulation of the hypothalamic-pituitary-adrenocortical (HPA) axis, including glucocorticoid receptors have been linked to ROS, pharmacological or genetic manipulations causing anxiety also impact memory and cognition [Izquierdo and Medina, 1999; Park et al., 2001; O'Shea et al., 2004; Venero et al., 2005]. Neuroinflammatory damage can prevent mice from eliciting normal responses to light/dark stimuli [Pascual et al., 2011]. Neuroinflammation and other neurodegenerative conditions are commonly associated with aging [McGeer and McGeer, 2004; Rollo, 200]. Therefore, behavioral regulation in response to changing environmental contexts (such as illumination) may be impaired in old mice. After testing in bright light, we repeated the circle run test and step-down test in dim illumination. In both tests, aging untreated mice showed virtually identical behaviors regardless of lighting. Conversely, behavioral responses of supplemented mice were significantly different in dim light compared to bright illumination. These results suggest that supplemented mice had better contextual discrimination implying stronger cognitive function. Indeed, our MDS was already shown to improve cognition of aging mice [Lemon et al., 2003, Aksenov et al., 2013]. Impaired light/dark discrimination was also associated with poor locomotor ability [McGeer and McGeer, 2004]. Our MDS was shown to upregulate locomotion in mice [Aksenov et al., 2010]. Taken together, it appears that our treatment has a general impact on brain sensorimotor neurocircuitry.

Visual Acuity

The principle behind tests of visual acuity involves challenging mice with increasingly more difficult visual cues and determining when correct responses are extinguished [Prusky et al., 2000]. Based on this, we developed a novel test from a less sensitive version [Chaudhry et al., 2008], which uses the animal's natural tendency to reach for perceived objects or surfaces to escape when suspended by the tail. We found that ~2-year-old Nr mice had largely intact vision as all animals successfully responded to repeated presentation of a distinct visual cue on high contrast background, irrespective of treatment. However, untreated mice showed a progressive loss of

Environmental and Molecular Mutagenesis. DOI 10.1002/em

reaching responses as increasingly more subtle visual cues were presented. In comparison, responses of supplemented mice extinguished at slower rates. Significant differences between supplemented and untreated mice were resolved on a moderately difficult visual challenge. These findings suggest that the MDS may offset visual acuity decline seen in ageing.

Histological examination of the retinas from 2-year-old Nr mice indicated markers of retinal morphology were found to be consistent with those of age-related retinal degeneration. The MDS was designed to target key mechanisms associated with aging which include: oxidative stress, inflammation, and mitochondrial function [Lemon et al., 2003]. The robust efficacy of our MDS on these parameters has been experimentally confirmed [Lemon et al., 2008a,b, Aksenov et al., 2010, 2013; Long et al., 2012]. Thicknesses of the retinal outer nuclear layer (ONL) and outer segment (OS) were increased by 26 and 29%, respectively in MDS mice, compared to untreated mice. Unfortunately due to the limited age-range of samples, it was not possible to determine the magnitude of retinal degeneration and the extent to which the retinal atrophy was salvaged by MDS supplementation. However, despite this limitation, the reduced retinal atrophy in MDS supplemented mice was likely the result of attenuated oxidative and inflammatory processes and boosted mitochondrial function. Irregular organization and degeneration of the ONL and OS organization are closely associated with age-related macular degeneration (AMD) in humans [Gartner and Henkind, 1981]. In mouse models for AMD, geographic atrophy of the ONL and OS are regarded as chief biomarkers of retinal degeneration consistent with human AMD [Kim et al., 2002, Rakoczy et al., 2002, Karan et al., 2005, Rakoczy et al., 2006, Justilien et al., 2007]. The ONL contains photoreceptor nuclei; thinning of the ONL occurs as a result of cell depletion with a reduction in associated photoreceptors, resulting in diminished visual acuity [Gartner and Henkind, 1981, Kim et al., 2002, Kashani et al., 2009]. Likewise, the OS reflect rod and cone abundance [Carter-Dawson and LaVail, 1979]. In this fashion, improved visual acuity in old supplemented mice is consistent with reduced retinal degeneration. Given that similar geographic atrophy is observed in AMD, it is arguable that our MDS may offset this pathology in humans. Although murine retinas do not possess macula, patterns of retinal degeneration in mice correspond to those in human macular degeneration, thus useful inferences can be drawn to human visual acuity [Rakoczy et al., 2002; Karan et al., 2005; Rakoczy et al., 2006; Edwards and Malek, 2007; Justilien et al., 2007; Chu et al., 2013]. Retinal degeneration results largely from dysregulation in multiple factors, however inflammatory processes and oxidative damage play key roles in the development of this pathology [Winkler et al., 1999; Hogg and Chakravarthy, 2004; Edwards and Malek, 2007, Hollyfield et al., 2008; Saski et al., 2009; Barot et al., 2011]. Studies investigating the use of antioxidants to prevent AMD had variable, yet promising success [Hogg and Chakravarthy, 2004; Van Leeuwen et al., 2005]. However, a recent review of clinical and experimental data concluded that singly administered antioxidants (such as vitamin E and β-carotene) did not improve AMD prognosis [Evans, 2008]. Recently, mitochondrial dysfunction was additionally implicated in development of AMD [Barot et al., 2011]. Considering that this pathology involves dysregulation of multiple cellular systems, greater therapeutic benefits should be possible through complex multi-targeted interventions.

Olfaction

Morphological changes in olfactory bulbs of aging rodents are somewhat debatable with respect to laminar features. Volume (or thickness) of GLM and EPL are normally used as measures of aging, however results have been inconsistent [Hinds and McNelly, 1977; Mirich et al., 2002; Richard et al., 2010]. Some report no significant changes in volumes with age [Richard et al., 2010], while others show that thickness of these layers (as well as the entire bulb volume) increases between 6 and 24 months [Mirich et al., 2002]. Increases appeared to be equally proportional in each layer [Mirich et al., 2002]. Hinds and McNelly [1977] observed that volumes of all laminar layers in rat olfactory bulbs significantly increased from 3 to 24 months of age, followed by a sharp decline thereafter. At oldest ages (~30 months) layer volumes were identical to those in 3–12 month old rats. Collectively, it appears that laminar volumes increase with age, if extremely old animals were excluded [Hinds and McNelly, 1977; Mirich et al., 2002]. The mice in the current study were aged 14–17 months, with MDS treatment resulting in significantly reduced volumes of the GLM and EPL. This suggested that MDS treatment offset age-related morphological changes, which was supported by the improved olfactory sensitivity in MDS treated aging mice.

Mitral cells are the primary output neurons in the olfactory bulb that process olfactory sensory input prior to activating higher-order processing [Meister and Bonhoeffer, 2001; Rawson, 2006]. Age-related (or otherwise caused) loss of odor perception may occur due to complications afferent to mitral cells, but mitral cell dysfunction is ultimately implicated [Meisami et al., 1998; Rawson, 2006]. Loss of mitral cells with age is documented in rodents [Hinds and McNelly 1977; Mirich et al., 2002] and sizable declines are also observed in humans [Bhatnager et al., 1987; Meisami et al., 1998]. Our MDS treated mice showed a 29% increase in mitral cells, suggesting MDS treatment protected these neurons from age-related atrophy. However, due to difficulty in morphological

discrimination of mitral cells from sections stained only with H&E, these preliminary results should be interpreted with caution. Mitral cells are particularly susceptible to oxidative and nitrosative stress [Vaishnav et al., 2007, Yang et al., 2013]. Amount of 3-NT (a marker for protein nitration) was significantly elevated in olfactory bulbs of old mice [Vaishnav et al., 2007; Yang et al., 2013]. 3-NT was evident in the mitral cell layer, but was also delocalized to the EPL and GLM in advanced ages [Vaishnav et al., 2007]. Previous studies on MDS treatment demonstrated significantly lowered 3-NT levels in brains of aging mice [Long et al., 2012] and protein carbonyls were also reduced [Aksenov et al., 2010], emphasizing the potential protective capacity of the MDS on the mitral cell population.

Olfaction and Neurodegenerative Disease in Humans

Humans, like other animals, display age-related declines in olfactory function [Cain and Stevens, 1989; Nakayasu et al., 2000; Rawson, 2006). Losing the sense of smell per se, does not pose a major threat for humans, although quality of life may be impacted [Rawson, 2006]. However, greater concerns emerged when loss of olfaction was found to be strongly correlated with the risk of developing severe neurodegenerative conditions [Wilcock and Esiri, 1982; Ohm and Braak, 1987]. Alzheimer's (AD) patients show deterioration of mitral cells, with substantial mitral cell loss apparent before clinical AD symptoms emerged [Struble and Clark, 1992]. Combined with previous reports of severe olfactory deficits in dementia, AD and Parkinson's disease (PD), authors suggested that olfactory dysfunction may be an early manifestation of neurodegenerative disease [Doty et al., 1989; Koss et al., 1989; Schiffman et al., 1990; Struble and Clark, 1992; Devanand et al., 2000; Schiffman et al., 2002; Li et al., 2010; Baba et al., 2012; Doty, 2012]. Neuronal loss and altered olfactory morphology was later shown in young AD patients [Ter Laak et al., 1994], suggesting that loss of olfaction and olfactory neurons is not simply an age-related condition that parallels cognitive impairment in old AD patients. In fact some have even proposed that pathogenesis in AD and PD may be catalyzed by agents that enter the brain via olfactory pathways [Doty, 2008]. The accuracy of olfactory tests in early detection of neural pathology suggests that individuals with intact sense of smell are at lower risk of developing neurodegenerative conditions in the near future. Higher counts of mitral cells in the olfactory bulb also reflect higher neuronal populations in adjacent brain regions. Given that aging supplemented mice showed better olfactory sensitivity and higher number of mitral cells in the olfactory bulb, may suggest that the MDS could be offsetting neurodegeneration throughout the brain.

CONCLUSION

Effects of treatment with a multi-ingredient dietary supplement designed to ameliorate key mechanisms of aging showed treatment was associated with reduced anxiety-like behaviors, augmented discrimination of environmental context, improved motor balance, and improved visual and olfactory acuity. This was correlated with positive morphological changes and higher neuronal populations in the cerebellum and olfactory bulb, increased overall brain cell numbers and improved brain function. Intact olfaction is strongly indicative of suppression of neuronal degeneration. Retinal atrophy (associated with AMD) was also diminished in supplemented mice. Given that MDS treatment has been shown to significantly reduce oxidative damage, boost mitochondrial function [Lemon et al 2008a,b; Aksenov et al., 2010; Aksenov et al., 2013] and alleviate symptoms of inflammation [Lemon et al., 2005], suggests that neuronal protection and sensory function are likely attributed to diminishing oxidative/inflammatory stress and improved energy balance. The extent of functional benefits attained by our MDS here and in earlier studies [Lemon et al., 2003, 2005, 2008a,b; Aksenov et al., 2010, 2013; Long et al., 2012; Hutton et al., 2015' strongly suggests that aging animals retain the capacity to support youthful phenotypes and that powerful impacts can be achieved through multi-ingredient dietary supplementation that addresses the multifactorial nature of aging organisms.

ACKNOWLEDGMENTS

The authors would like to recognize that JA Lemon and V Aksenov contributed equally to both writing of this manuscript and collecting/analyzing data presented in this work. Olfactory sensitivity was tested by R Samigullina, while S Aksenov contributed majorly to histological analysis of retina, cerebellum and olfactory bulb. Special thanks to Ted A. Aristilde for providing technical histology support and Dr. Henry Szechtman for providing the image tracking system for behavioral studies and the expert technical assistance from Sarah Laronde, Mary Ellen Cybulski and Dale.

REFERENCES

Aksenov V, Long J, Lokuge S, Foster JA, Liu J, Rollo CD. 2010. Dietary amelioration of locomotor, neurotransmitter and mitochondrial aging. Exp Biol Med 235:66–76.

Aksenov V, Long J, Liu J, Szechtman H, Khanna P, Matravadia S, Rollo CD. 2013. A complex dietary supplement augments spatial learning, brain mass, and mitochondrial electron transport chain activity in aging mice. Age 35:23–33.

Andersen BB, Gundersen HJG, Pakkenberg B. 2003. Aging of the human cerebellum: A stereological study. J Compar Neurol 466: 156–365.

Antier D, Carswell HV, Brosnan MJ, Hamilton CA, Macrae IM, Groves S, Jardine E, Reid JL, Dominiczak AE. 2004. Increased levels of

superoxide in brains from old female rats. Free Radic Res 38: 177–182.

Apps R, Garwicz M. 2005. Anatomical a physiological foundations of cerebellar information processing. Nat Rev Neurosci 6:297–311.

Baba T, Kikuchi A, Hirayama K, Nishio Y, Hosokai Y, Kanno S, Hasegawa T, Sugeno N, Konno M, Suzuki K, et al., 2012. Severe olfactory dysfunction is a prodromal syndrome of dementia associated with Parkinson's disease: A 3 year longitudinal study. Brain 135:161

Balaban CD. 2002. Neural substrates linking balance control and anxiety. Physiol Behav 77:469–475.

Balaban CD, Jacob RG, Furman JM. 2011. Neurologic bases for comorbidity of balance disorders, anxiety disorders and migraine: neurotheraputic implication. Expert Rev Neurotheraputics 11:379–394.

Barot M, Gokulgandi R, Mitra AK. 2011. Mitochondrial dysfunction in retinal diseases. Curr Eye Res 36:1069–1077.

Barski JJ, Dethleffsen K, Meyer M. 2000. Cre recombinase expression in cerebellar Purkinje cells. Genesis 28:93–98.

Barski JJ, Hartmann J, Rose CR, Hoebeek F, Mörl K, Noll-Hussong M, De Zeeuw CI, Konnerth A, Meyer M. 2003. Calbindin in the cerebellar Purkinje cells is a critical determinant of the precision of motor coordination. J Neurosci 23:3469–3477.

Bartke A, Chandrashekar V, Bailey B, Zaczek D, Turyn D. 2002. Consequences of growth hormone (GH) overexpression and GH resistance. Neuropep 36:201–208.

Bartke A. 2003. Can growth hormone (GH) accelerate aging? Evidence from GH-transgenic mice. Neuroendocrinol 78:210–216.

Beekman ATF, Bremmer MA, Deeg DJH, Van Balkom AJLM, Smit JH, De Beurs E, Dyck RV, Van Tilburg W. 1998. Anxiety disorders in later life: A report from the longitudinal aging study Amsterdam. Int J Geriat Psych 13:717–726.

Beierlein M. 2014. Synaptic mechanisms underlying cholinergic control of thalamic reticular nucleus neurons. J Physiol 592:4137–4145.

Belzung C, Griebel G. 2001. Measuring normal and pathological anxiety-like behavior in mice: A review. Behav Brain Res 125: 141–149.

Berry A, Capone F, Giorgio M, Pelicci PG, De Kloet ER, Alleva E, Minghetti L, Cirulli F. 2007. Deletion of the life span determinant p66Sch prevents age-related dependant increase in emotionality and pain sensitivity in mice. Exp Geront 42:37–45.

Bercik P, Verdu EF, Foster JA, Marci J, Potter M, Huang X, Malinowski P, Jackson W, Blennerhassett P, Neufeld KA, et al., 2010. Chronic gastrointestinal inflammation induces anxiety-like behavior and alters nervous system biochemistry in mice. Gastroenterol 139:2102–2112.

Bhatnagar KP, Kennedy RC, Baron G, Greenberg RA. 1987. Number of mitral cells and the bulb volume in the aging human olfactory bulb: A quantitative morphological study. Anat Record 218:73–78.

Bickford PC, Shukitt-Hale B, Joseph J. 1999. Effects of aging on cerebellar noradrenergic function and motor learning: Nutritional interventions. Mech Ageing Dev 111:141–154.

Bobée S, Mariette E, Tremblay-Leveau H, Caston J. 2000. Effects of early midline cerebellar lesion on cognitive and emotional functions in the rat. Behav Brain Res 112:107–117.

Bouayed J, Rammal H, Soulimani R. 2009. Oxidative stress and anxiety: Relationship and cellular pathways. Oxid Med Cell Longev 2:63–67.

Bratic A, Larsson NG. 2013. The role of mitochondrial in aging. J Clin Invest 123:951–957.

Butterfield DA. 2014. The 2013 SFRBM discovery award: Selected discoveries from the butterfield laboratory of oxidative stress and its sequela in brain in cognitive disorders exemplified by Alzheimer disease and chemotherapy induced cognitive impairment. Free Radic Biol Med 74:157–174.

Butterfield DA, Howard BJ, LaFontaine MA. 2001. Brain oxidative stress in animal models of accelerated aging and the age-related neurodegenerative disorders, Alzheimer's disease and Huntington's disease. Curr Med Chem 8:815–828.

Cain WS, Stevens JC. 1989. Uniformity of olfactory loss in aging. Ann NY Acad Sci 561:29–38.

Calder WA. 1984. Size, Function and Life History. Cambridge: Harvard University Press. 431 p.

Carlson JC, Bharadwaj R, Bartke A. 1999. Oxidative stress in hypopituitary dwarf mice and in transgenic mice overexpressing human and bovine GH. Age 22:181–186.

Carola V, D'Olimpio F, Brunamonti E, Mangia F, Renzi P. 2002. Evaluation of the elevated plus-maze and open-field tests for the assessment of anxiety-related behaviour in inbred mice. Behav Brain Res 134:49–57.

Carter RJ, Morton J, Dunnett SB. 2001. Motor coordination and balance in rodents. Curr Protoc Neurosci. Chapt 8:Unit 8.12.

Carter-Dawson LD, LaVail MM. 1979. Rods and cones in the mouse retina. J Comp Neur 188:245–262.

Chaudhry AM, March-Rollo SE, Aksenov V, Rollo CD, Szechtman H. 2008. Modifier selection by transgenesis: The case of growth hormone transgenic and hyperactive circling mice. Evol Biol 35: 267–286.

Choi D, Furay A, Evanson N, Ostrander M, Ulrich-Lai Y, Herman J. 2007. Bed nucleus of the stria terminalis subregions differentially regulate hypothalamic–pituitary–adrenal axis activity: Implications for the integration of limbic inputs. J Neurosci 27:2025–2034.

Chung HY, Sung B, Jung KJ, Zou Y, Yu BP., 2006 The molecular inflammatory processes in aging. Antioxid Redox Sign 8:572–581.

Cohen G, Farooqui R, Kesler N. 1997. Parkinson disease: A new link between monoamine oxidase and mitochondrial electron flow. Proc Natl Acad Sci USA 94:4890–4894.

Colucci-Guyon E, Ribotta MGY, Maurice T, Babinet C, Privat A. 1999. Cerebelar defect and impaired motor coordination in mice lacking vimentin. Glia 25:33–43.

Cui H, Kong Y, Zhang Y. 2012. Oxidative stress, mitochondrial dysfunction, and aging. J Signal Transduct 2012:646354

Dahhaoui M, Lannou J, Stelz T, Caston J, Guastavina JM. 1992. Role of the cerebellum in spatial orientation of the rat. Behav Neural Biol 58:180–189.

D'Angelo E. 2012. Cerebellar Granule Cell. In: Manto M, Schmahmann JD, Rossi F, Gruol DL, Koibuchi N, editors. Handbook of the Cerebellum and Cerebellar Disorders. Netherlands: Springer. pp 765–791.

D'Angelo E, De Zeeuw CI. 2009. Timing and plasticity on the cerebellum: Focus on the granular layer. Trends Neurosci 32:30–40.

Dei R, Takeda A, Niwa H, Li M, Nakagomi Y, Watanabe M, Inagaki T, Washimi Y, Yasuda Y, Horie K, et al., 2002. Lipid peroxidation and advanced glycation end products in the brain in normal aging and in Alzheimer's disease. Acta Neuropathol (Berl) 104:113–122.

De Oliveira MR, Silvestrin RB, Mello E, Souza T, Moreira JC. 2007. Oxidative stress in the hippocampus, anxiety-like behavior and decreased locomotory and exploratory activity of adult rats: Effects of subacute vitamin A supplementation at therapeutic doses. Neurotoxicol 6:1191–1199.

Devanand DP, Michaels-Marston KS, Liu X, Pelton GH, Padilla M, Marder K, Bell K, Stern Y, Mayeux R. 2000. Olfactory deficits in patients with mild cognitive impairment predict Alzheimer's disease at follow-up. Am J Psychiatry 157:1399–1405.

Doty RL. 2008. The olfactory vector hypothesis of neurodegenerative disease: is it viable? Ann Neurol 63:7–15.

Doty RL. 2012. Olfactory dysfunction in Parkinson's disease. Nat Rev Neurol 8:329–339.

Doty RL, Riklan M, Deems DA, Reynolds C, Stellar S. 1989. The olfactory and cognitive deficits of Parkinson's disease: Evidence for independence. Ann Neurol 25:166–171.

Doulazmi M, Frédéric F, Lemaigre-Debreuil Y, Hadj-Sahraoui N, Delhaye-Bouchard N, Mariani J. 1999. Cerebellar purkinje cell loss during life span of the heterozygous Staggerer mouse (Rora+/Rorasg) is gender related. J Compar Neurol 411:267–273.

Droge W. 2002. Free radicals in the physiological control of cell function. Physiol Rev 82:47–95.

Du F, Zhu XH, Zhang Y, Friedman M, Zhang N, Uğurbil K, Chen W. 2002. Tightly coupled brain activity and cerebral ATP metabolic rate. Proc Natl Acad Sci USA 105:6409–6414.

Edwards AO, Malek G. 2007. Molecular genetics of AMD and current animal models. Angiogen 10:119–132.

Erecinska M, Cherian S, Silver IA. 2004. Energy metabolism in mammalian brain during development. Prog Neurobiol 73:397–445.

Evans J. 2008. Antioxidant supplements to prevent or slow down the prognosis of AMD: A systemic review and meta-analysis. Eye 22:751–760.

Finkel T, Holbrook NJ. 2012 Oxidants, oxidative stress and the biology of ageing. Nature 408:239–247.

Foster MJ, Dubey A, Dawson KM, Stutts WA, Lal H, Sohal RS. 1996. Age-related losses of cognitive function and motor skills in mice are associated with oxidative protein damage in the brain. Proc Natl Acad Sci USA 93:4765–4769.

Gandhi S, Abramov AY. 2012. Mechanism of oxidative stress in neurodegeneration. Oxid Med Cell Longev 2012:428010

Gartner S, Henkind P. 1981. Aging and degeneration of the human macula. I. Outer nuclear layer and photoreceptors. Brit J Ophthalmol 65:32–28.

Ghelarducci B, Salamone D, Simoni A, Sebastiani L. 1996. Effects of early cerebellar removal on the classically conditioned bradycardia of adult rabbits. Exp Brain Res 111:417–423.

Girardi M, Konrad HR, Amin M, Hughes LF. 2001. Predicting fall risks in an elderly population: Computer dynamic posturography versus electronystagmography test results. Laringoscope 111:1528–1532.

Grimm S, Hoehn A, Davies KJ, Grune T. 2011. Protein oxidative modifications in the ageing brain: Consequence for the onset of neurodegenerative disease. Free Radic Res 45:73–88.

Hattingen E, Magerkurth J, Pilatus U, Mozer A, Seifried C, Steinmetz H, Zanella F, Hilker R. 2009. Phosphorus and proton magnetic resonance spectroscopy demonstrates mitochondrial dysfunction in early and advanced Parkinson's disease. Brain 132:3285–3297.

Hauck SJ, Bartke A. 2001. Free radical defenses in the liver and kidney of human growth hormone transgenic mice: Possible mechanisms of early mortality. J Geront 56:B153–B162. A:

Hinds JW, McNelly NA. 1977. Aging of the rat olfactory bulb: growth and atrophy of constituent layers and changes in size and number of mitral cells. J Comp Neurol 171:345–368.

Hogg R, Chakravarthy U. 2004. AMD and micronutrient antioxidants. Curr Eye Res 29:387–401.

Hollyfield JG, Bonihla VL, Rayborn ME, Yang X, Shadrach KG, Lu L, Urfet RL, Salomon RG, Perez VL. 2008. Oxidative damage-induced inflammation initiates age-related macular degeneration. Nat Med 14:194–198.

Huang C, Brown N, Huang RH. 1999. Age-related changes in the cerebellum: Parallel fibers. Brain Res 840:148–152.

Ikeyama S, Kokkonen G, Shack S, Wang XT, Holbrook NJ. 2002. Loss in oxidative stress tolerance with aging linked to reduced extracellular signal-regulated kinase and Akt kinase activities. FASEB 16:114–116.

Ito M. 2000. Mechanisms of motor learning in the cerebellum. Brain Res 886:237–245.

Izquierdo I, Medina JH. 1999 GABAA receptor modulation of memory: The role of endogenous benzodiazepines. Trends Pharmacol Sci 12:260–265.

Janssen YM, Houten B, Borm PJ, Mossman BT. 1993. Cells and tissue responses to oxidative damage. Lab Invest J Tech Method Pathol 69:261–274.

Justilien V, Pang JJ, Renganathan K, Zhan X, Crabb JW, Kim SR, Sparrow JR, Hauswirth WW, Lewin AS. 2007. SOD2 knockdown mouse model of early AMD. Invest Ophthalmil Vis Sci 48:4407–4420.

Kannurpatti SS, Sanganahalli BG, Mishra S, Joshi PG, Joshi NB. 2004. Glutamate-induced differential mitochondrial response in young and adult rats. Neurochem Int 44:361–369.

Karan G, Lillo C, Yang Z, Cameron DJ, Locke KG, Zhao Y, Thirumalaichary S, Li C, Birch DG, Vollmer-Snarr HR, et al., 2005. Lipofuscin accumulation, abnormal electrophysiology and photoreceptor degeneration in mutant ELOVL4 transgenic mice: a model for macular degeneration. Proc Natl Acad Sci 102:4161–4169.

Kashani AH, Keane PA, Dustin L, Walsh AC, Sadda SR. 2009. Quantitative subanalysis of cystoid spaces and outer nuclear layer using optical coherence tomography in age-related macular degeneration. Invest Ophthalmil Vis Sci 50:3366–3373.

Kashiwabuchi N, Ikeda K, Araki K, Hirano T, Shibuki K, Takayama C, Inoue Y, Kutsuwada T, Yagi T, Kang Y, et al., 1995. Impairment of motor coordination, Purkinje cell synapse formation, and cerebellar long-term depression in GluRδ2 mutant mice. Cell 81:245–252.

Keller JN, Pang Z, Geddes JW, Begley JG, Germeyer A, Waeg G, Mattson MP. 1997. Impairment of glucose and glutamate transport and induction of mitochondrial oxidative stress and dysfunction in synaptosomes by amyloid β-peptide: Role of the lipid peroxidation product 4-hydroxynonenal. J Neurochem 69:273–284.

Kim SY, Sadda S, Pearlman J, Humayun MS, de Huan E, Jr., Melia BM, Green WR. 2000. Morphometric analysis of the macula in eyes with discoform age-related macular degeneration. Retina 22: 471–477.

Koss E, Weiffenbach JM, Haxby JV, Friedland RP. 1988. Olfactory detection and identification performance in early Alzheimer's disease. Neurology 38:1228–1232.

Landis S. 1973. Ultrastructural changes in the mitochondria of cerebellar Purkinje cells of nervous mutant mice. J Cell Biol 57:782–797.

Larsen JO, Skalicky M, Viidik A. 2000. Does long-term physical exercise counteract age-related Purkinje cell loss? A stereological study of rat cerebellum. J Compar Neurol 428:213–222.

Lavrovsky Y, Chatterjee B, Clark RA, Roy AK. 2000. Role of redox-regulated transcription factor in inflammation, aging and age-related diseases. Exp Gerontol 35:521–532.

Lemon JA, Boreham DR, Rollo CD. 2003. A dietary supplement abolishes age-related cognitive decline in transgenic mice expressing elevated free radical processes. Exp Biol Med 228:800–810.

Lemon JA, Boreham DR, Rollo CD. 2005. A complex dietary supplement extends longevity of mice. J Gerontol A Biol Sci Med Sci 60:275–279.

Lemon JA, Rollo CD, McFarlane NM, Boreham DR. 2008a. Radiation-induced apoptosis in mouse lymphocytes is modified by a complex dietary supplement: The effect of genotype and gender. Mutagenesis 23:465–471.

Lenaz G. 1998. Role of mitochondria in oxidative stress and ageing. Biochim Biophys Acta 1366:53–67.

Li W, Howard JD, Gottfried JA. 2010. Disruption of odor quality coding in piriform cortex mediates olfactory deficits in Alzheimer's disease. Brain 133:2714–2726.

Long J, Aksenov V, Rollo CD, Liu J. 2012. A complex dietary supplement modulates nitrative stress in normal mice and in a new

mouse model of nitrative stress and cognitive aging. Mech Ageing Devel 133:523–529.

Lyras L, Cairns NJ, Jenner A, Jenner P, Halliwell B. 1997. An assessment of oxidative damage to proteins, lipids, and DNA in brains from patients with Alzheimer's disease. J Neurochem 68:2061–2069.

Ma L, Morton AJ, Nicholson LF. 2003. Microglia density decreases with age in a mouse model of Huntington's disease. Glia 43: 274–280.

Markesbury WR, Carney JM. 1999. Oxidative alterations in Alzheimer's disease. Brain Pathol 9:133–146.

Masood A, Nadeem A, Mustafa SJ, O'Donnell JM. 2008. Reversal of oxidative stress-induced anxiety by inhibition of phosphodiesterase-2 in mice. J Pharm Exp Ther 326:369–379.

Mattson MP, Pedersen WA, Duan W, Culmsee C, Camandola S. 1999. Cellular and molecular mechanisms underlying perturbed energy metabolism and neuronal degeneration in Alzheimers and Parkinson's diseases. Ann NY Acad Sci 893:154–175.

Mattson MP, Magnus T. 2004 Ageing and neuronal vulnerability. Nat Rev Neurosci 7:278–294.

Maurya PK, Noto C, Rizzoa LB, Riosa AC, Nunes SOV, Barbosa DS, Sethi S, Zeni M, Mansur RB, et al., 2016. The role of oxidative and nitrosative stress in accelerated aging and major depressive disorder. Prog Neuropsychopharmacol Biol Psychiatry 65:134–144.

McGeer PL, McGeer EG. 2004. Inflammation and the degenerative diseases of aging. Ann NY Acad Sci 1035:104–116.

Meisami E, Mikhail L, Baim D, Bhatnagar KP. 1998. Human olfactory bulb: Aging of glomeruli and mitral cells and a search for the accessory olfactory bulb. Ann NY Acad Sci 855:708–715.

Meister M, Bonhoeffer T. 2001. Tuning and topography in an odor map on the rat olfactory bulb. J Neurosci 21:1351–1360.

Meliska CJ, Burke PA, Bartke A, Jensen RA. 1997. Inhibitory avoidance and appetitive learning in aged normal mice: comparison with transgenic mice having elevated plasma growth hormone levels. Neurobiol Learn Mem 68:1–12.

Mirich JM, Williams NC, Berlau DJ, Brunjes PC. 2002. Comparative study of aging in the mouse olfactory bulb. J Comp Neurol 454: 361–372.

Mitchell AS. 2015. The mediodorsal thalamus as a higher order thalamic relay nucleus important for learning and decision-making. Neurosci Biobehav Rev 54:76–88.

Monfort V, Chapillon P, Mellier D, Lalonde R, Caston J. 1998. Time active avoidance learning in lurcher mutant mice. Behav Brain Res 91:165–172.

Mutlu-Turkoglu U, Ilhan E, Oztezcan S, Kuru A, Aykac-Toker G, Uysal M. 2003. Age-related increases in malondialdehyde and protein carbonyl levels and lymphocyte DNA damage in elderly patients. Clin Biochem 36:397–400.

Nakayasu C, Kanemura F, Hirano Y, Shimizu Y, Tonosaki K. 2000. Sensitivity of olfactory sense declines with the aging in senescence-accelerated mouse (SAM-P1). Physiol Behav 70:135–139.

Nakamura T, Lipton SA. 2007. Molecular mechanisms of nitrosative stress-mediated protein misfolding in neurodegenerative diseases. Cell Mol Life Sci 64:1609–1620.

NK, Yadollah A. MM, 2009. Chronic inflammation and oxidative stress as a major cause of age-related diseases and cancer. Recent Pat Inflamm Allergy Drug Discov 3:73–80.

Ogueta S, Olazabal I, Santos I, Delgado-Baeza E, Garcia-Ruiz JP. 2000. Transgenic mice expressing bovine GH develop arthritic disorder and self-antibodies. J Endocrinol 165:321–328.

Ohm TG, Braak H. 1987. Olfactory bulb changes in Alzheimer's disease. Acta Neuropathol 73:365–369.

O'Shea M, Singh ME, McGregor IS, Mallet PE. 2004. Chronic cannabinoid exposure produces lasting memory impairment and increased anxiety in adolescent but not adult rats. J Psychopharmacol 18:502–508.

Palmiter RD, Brinster RL, Hammer RE. 1982. Dramatic growth of mice that develop from eggs microinjected with metallothionein–growth hormone fusion genes. Nature 300:611–615.

Park CR, Campbell AM, Diamond DM. 2001. Chronic psychological stress impairs learning and memory and increases sensitivity to Yohimbine in adult rats. Biol Psychiatry 50:994–1004.

Parrish-Aungst S, Shipley MT, Erdelyi F, Szabo G, Puche AC. 2007. Quantitative analysis of neuronal diversity in the mouse olfactory bulb. J Comp Neurol 501:825–836.

Pascual M, Baliño P, Alfonso-Loeches S, Aragón CMG, Guerri C. 2011. Impact of LTR4 on behavioral and cognitive dysfunctions associated with alcohol-induced neuroinflammatory damage. Brain Behav Immun 25:S80–S90.

Paulin MG. 1993. The role of the cerebellum in motor control and perception. Brain Behav E 41:39–50.

Prusky GT, West PWR, Douglas RM. 2000. Behavioral assessment of visual acuity in mice and rats. Vision Res 40:2201–2209.

Rakoczy PE, Yu MJT, Nusinowitz S, Chang B, Heckenlively JR. 2006. Mouse models of age-related macular degeneration. Exp Eye Res 82:741–752.

Rakoczy PE, Zhang D, Robertson T, Barnet NL, Papadimitriou J, Constable IJ, Lai CM. 2002. Progressive age-related changes similar to age-related macular degeneration in a transgenic mouse model. Am J Pathol 161:1515–1524.

Rawson NE. 2006. Olfactory loss in aging. Sci Aging Knowl Environ pe6

Reddy PH, Beal MF. 2008. Amyloid beta, mitochondrial dysfunction and synaptic damage: implications for cognitive decline in aging and Alzheimer's disease. Trends Mol Med 14:45–53.

Reuter S, Gupta SC, Chaturvedi MM, Aggarwal BB. 2010. Oxidative stress, inflammation and cancer: how are they linked? Free Radic Biol Med 49:1603–1616.

Richard MB, Taylor SR, Greer CA. 2010. Age-induced disruption of selective olfactory bulb synaptic circuits. Proc Natl Acad Sci USA 107:15613–15618.

Rogers J, Zornetzer AF, Bloom FB, Mervis RE. 1984. Senescent microstructural changes in rat cerebellum. Brain Res 292:23–32.

Rollo CD, Carlson J, Sawada M. 1996. Accelerated aging of giant transgenic growth hormone mice is associated with elevated free radical processes. Can J Zoo 74:606–620.

Rollo CD, Ko CV, Tyerman JGA, Kajiura L. 1999. The growth hormone axis and cognition: empirical results and integrated theory derived from giant transgenic mice. Can J Zoo 77:1874–1890.

Rollo CD. 2002 Growth negatively impacts the life span of mammals. Evol Dev 4:55–61.

Sakaguchi A, Katamine S, Nishida N, Moriuchi R, Shigematsu K, Sugimoto T, Nakatani A, Kataoka Y, Houtani T, Shirabe S, et al., 1996. Loss of cerebellar Purkinje cells in aged mice homozygous for a disrupted PrP gene. Nature 380:528–531.

Salim S, Sarraj N, Taneja M, Saha K, Tajeda-Simon MV, Chugh G. 2010. Moderate treadmill exercise prevents oxidative stress-induced anxiety-like behavior in rats. Behav Brain Res 208:545–552.

Sasaki M, Ozawa Y, Kurihara T, Noda K, Imamura Y, Kobayashi S, Ishida S, Tsubota K. 2009. Neuroprotective effect of an antioxidant, lutein, during retinal inflammation. Invest Ophthalmol Vis Sci 50:1433–1439.

Sastre J, Pallardo FV, Vina J. 2003. The role of mitochondrial oxidative stress in aging. Free Rad Biol Med 35:1–8.

Savory J, Rao JKS, Huang Y, Letada PR, Herman MM. 1999. Age-related hippocampal changes in Bcl-2:Bax ratio, oxidative stress, redox-active iron and apoptosis associated with aluminium-induced neurodegeneration: increased susceptibility with aging. Neurotox 20:805–818.

Schiffmann SN, Cheron G, Lohof A, d'Alcantara P, Meyer M, Parmentier M, Schurmans S. 1999. Impaired motor coordination and Purkinje cell excitability in mice lacking calretinin. Proc Natl Acad Sci USA 96:5257–5262.

Schiffman SS, Clark CM, Warwick ZS. 1990. Gustatory and olfactory dysfunction in dementia: not specific to Alzheimer's disease. Neurobiol Aging 11:597–600.

Schiffman SS, Graham BG, Sattely-Miller EA, Zervakisa J, Welsh-Bohmera K. 2002. Taste, smell and neuropsychological performance of individuals at familial risk for Alzheimer's disease. Neurobiol Aging 23:397–404.

Schmahmann JD, Caplan D. 2006. Cognition, emotion and the cerebellum. Brain 129:290–292.

Schutter DJLG Van Honk J. 2005. The cerebellum on the rise in human emotion. Cerebellum 4:290–294.

Shigenaga MK, Hagen TM, Ames BN. 1994. Oxidative damage and mitochondrial decay in aging. Proc Natl Acad Sci USA 91: 10771–10778.

Sidman RL, Green MC. 1970. Nervous, a new mutant mouse with cerebellar disease. In: Sabourdy M, editor. Les mutants pathologiques chez l'animal, leur intérêt dans la recherché biomédicale. CNRS, Paris:CNRS.

Song C, Li X, Leonard BE, Horrobin DF. 2003. Effects of dietary n-3 or n-6 fatty acids on interleukin-1β-induced anxiety, stress, and inflammatory responses in rats. J lipid Res 44:1984–1991.

Sonta T, Inoguchi T, Tsubouchi H, Sekiguchi N, Matsumoto S, Utsumi H, Nawata H. 2004. Evidence for contribution of vascular NAD(P)H oxidase to increased oxidative stress in animal models of diabetes and obesity. Free Radic Biol Med 37:115–123.

Spear PD. 1993. Neural bases of visual deficits during aging. Vis Res 33:2589–2609.

Steger RW, Bartke A, Cecim M. 1993. Premature aging in transgenic mice expressing different growth hormone genes. J Reprod Fert 46:61–75.

Struble RG, Clark HB. 1992 Olfactory bulb lesions in Alzheimer's disease. Neurobiol Aging 13:469–473.

Szechtman H. 1988. Effects of dopamine receptor agonist apomorphine on sensory input. Naunyn-Schmiedeberg's Arch Pharmacol 338: 489–496.

Tan JSL, Wang JJ, Liew G, Rochtchina E, Mitchell P. 2008. Age-related macular degeneration and mortality from cardiovascular disease or stroke. Br J Ophthalmol 92:509–512.

Ter Laak HJ, Renkawek K, Van Workum FPA. 1994. The olfactory bulb in Alzheimer's disease: A morphologic study of neuron loss, tangles, and senile plaques in relation to olfaction. Alz. Dis Assoc Dis 8:38–48.

Tong G, Robertson LT, Brons J. 1993. Climbing fiber representation of the renal afferent nerve in the vermal cortex of the cat cerebellum. Brain Res 607:65–75.

Trullas R, Skolnick P. 1993. Differences in fear motivated behaviors among inbred mouse strains. Psychopharm 111:323–331.

Vaishnav RA, Getchell ML, Poon HF, Barnett KR, Hunter SA, Pierce WM, Klein JB, Butterfield DA, Getchell TV. 2007. Oxidative stress in the aging murine olfactory bulb: Redox proteomics and cellular localization. J Neurosci Res 85:373–385.

Van Leeuwen R, Boekhoorn S, Vingerling JR, Witteman JCM, Klaver CCW, Hofman A., De Jong PTVM 2005. Dietary intake of antioxidants and age-related macular degeneration. JAMA 294:3101–3107.

Venero C, Guadaño-Ferraz A, HAI, Nordström K, Manzano J, De Escobar GM, Bernal J., Vennström B, 2005. Anxiety, memory impairment, and locomotor dysfunction caused by a mutant thyroid hormone receptor α1 can be ameliorated by T3 treatment. Genes Dev 19:2152–2163.

Voikar V, Kõks S, Vasar E, Rauvala H. 2001. Strain and gender differences in the behavior of mouse lines commonly used in transgenic studies. Physiol Behav 72:271–281.

von Bohlen und Halbach O, Unsicker K. 2002. Morphological alterations in the amygdala and hippocampus of mice during ageing. Eur J Neurosci 16:2434–2440.

Wallace JE, Krauter EE, Campbell BA. 1980. Motor and reflective behavior in the aging rat. J Gerontol 35:364–370.

Wang X, Michaelis EK. 2010. Selective neuronal vulnerability to oxidative stress in the brain. Front Aging Neurosci 2:12

Weimer JM, Benedict JW, Getty AL, Pontikis CC, Lim MJ, Cooper JD, Pearce DA. 2009. Cerebellar defects in a mouse model of juvenile neuronal ceroid lipofuscinosis. Brain Res 1266:93–107.

Wilcock GK, Esiri MM. 1982. Plaques, tangles and dementia. A quantitative study. J Neurol Sci 56:342–356.

Winkler BS, Boulton ME, Gottsch JD, Sternberg P. 1999. Oxidative damage and age-related macular degeneration. Mol Vis 5:32

Witt RM, Galligan MM, Despinoy JR, Segal R. 2009. Olfactory behavioral testing in the adult mouse. J Vis Exp 23:949.

Wolf E, Kahnt E, Ehrlein J, Hermanns W, Brem G, Wanke R. 1993. Effects of long-term elevated serum levels of growth hormone on life expectancy of mice: Lessons from transgenic animal models. Mech Ageing Dev 68:71–87.

Wolf OT. HPA axis and memory. Best Pract Res Cl En 17:287–299.

Woodruff-Pak DS. 2006. Stereological estimation of Purkinje neuron number in C57BL/6 mice and its relation to associative learning. Neuroscience 141:233–243.

Woodruff-Pak DS, Foy MR, Akopian GG, Lee KH, Zach J, Nguyen KPT, Comalli DM, Kennar JA, Agelan A, Thompson RF. 2010. Differential effects and rates of normal aging in cerebellum and hippocampus. Pnas 107:1624–1629.

Wulff P, Schonewille M, Renzi M, Viltono L, Sassoè-Pognetto M, Badura A, Gao Z, Hoebeek FE, van Dorp S, Wisden W, et al., 2009. Synaptic inhibition of Purkinje cells mediates consolidation of vestibule-cerebellar motor learning. Nature Neurosci 12:1042–1049.

Yan MH, Wang X, Zhua X. 2013. Mitochondrial defects and oxidative stress in Alzheimer disease and Parkinson disease. Free Radic Biol Med 62:90–101.

Yang MJ, Sim S, Jeon JH, Jeong E, Kim HC, Park YJ, Kim IB. 2013. Mitral and tufted cells are potential cellular targets of nitration in the olfactory bulb of age mice. PLoS One 8:e59673

Yin F, Boveris A, Cadenas E. 2014. Mitochondrial energy metabolism and redox signaling in brain aging and neurodegeneration. Antiox Redox Signal 20:353–371.

AQ1: Please provide complete details for the affiliations.

AQ2: Please provide all author names in the list.

AQ3: Please confirm that given names (red) and surnames/family names (green) have been identified correctly.